PROTEIN-PROTEIN AND PROTEIN-DNA INTERACTIONS OF THE B/HLH/Z TRANSCRIPTION FACTORS MYC/MAX/MAD

By

Jianzhong Hu

A dissertation submitted to the Graduate Faculty in Biochemistry

in partial fulfillment of the requirements for the degree of

Doctor of Philosophy, The City University of New York

2004

This manuscript has been read and accepted for the Graduate Faculty in Biochemistry in satisfaction of the dissertation requirement for the degree of Doctor of Philosophy.

[required signature]

1/27/2004 _____
Date

_____
Chair of Examining Committee

[required signature]

2/6/2004 _____
Date

_____
Executive Officer

[typed name]

_____

[typed name]

_____

[typed name]

_____

[typed name]

_____
Supervisory Committee

THE CITY UNIVERSITY OF NEW YORK

ABSTRACT

Protein-protein and protein-DNA interactions of the b/HLH/z transcription factors Myc/Max/Mad

By

Jianzhong Hu

Adviser: Professor Dixie Goss

In the Myc/Max/Mad network, Max and Myc form a heterodimer that has strong oncogenic potential, while Mad and Max form a heterodimer that acts as a tumor suppressor. The mechanism of the transcription function of Myc/Max/Mad network is directly related to the interaction between these protein dimers and their DNA recognition site, a DNA E-box element, CACGTG. The quantitative data on these interactions does not clearly illustrate the binding mechanism. Fluorescence anisotropy has been used in our experimental approach to measure protein-protein and protein-DNA binding affinity. The enthalpy and entropy of these interactions were determined from the temperature dependence. The Max homodimer binds to the DNA with higher affinity than Myc/Max or Mad/Max heterodimers, but has less specificity for the E-box and flanking sequence recognition. The overall ΔG^{o} for formation of the protein dimer-DNA complex was almost 4 kJ less favorable for Mad-Max-DNA formation at 20°C compared to Max_2-DNA or Myc-Max-DNA, which were essentially the same. However, at 37°C Mad-Max-DNA and Myc-Max-DNA have essentially the same ΔG^{o} while Max_2-DNA was about 7

kJ less stable. The enthalpy values for Max_2-DNA formation were significantly higher than for either of the heterodimer-DNA interactions. The largest contribution was assigned to the protein-DNA interaction rather than the protein-protein interaction. These results suggest that the formation of heterodimers between Max and other proteins are a more important function of Max than the selection of DNA sequences. The fluorescence anisotropy measurement also suggests that for the unphosphorylated Max, the dimerization and protein-DNA interaction pathway might be favorable to the formation of Max monomer-DNA complex, instead of the formation of Max heterodimer. This result is consistent with the idea, that the Max phosphorylation by Casein Kinase II is the core upstream regulation of the entire Myc/Max/Mad network. This regulation affects the Max binding affinity with E-Box DNA. In Addition, the fluorescence resonance energy transferring (FRET) experiment on the protein-DNA interaction did not show significant difference between Myc/Max and Mad/Max heterodimer, interacting with E-box oligonucleotides. It might suggest that those heterodimers bind to the DNA with similar orientations, or if the orientation were different in vivo, there has to be some other factors involved.

ACKNOWLEDGMENTS

In this moment, first, I want to express my appreciation to my advisor, Dixie Goss, for the source of knowledge, guidance, and support that she has been to me over the past years. Her encouragement of my work and commitment to whatever project we would undertake was inspiring, and has made the time I have spent here enjoyable. I could not have had a better advisor and colleague. Also many thanks to all those who made this project possible by their support, especially to my colleagues and friends, Ms. Anamika Banerjee, Dr. John Trujillo, Dr. Diana Friedland, and other members in Dr. Goss' research group for their help and advice all the time.

Also I need to thank my parents and parents in law for encouraging and assisting me constantly, especially in attaining this degree. Their belief in me has helped during times when I have doubted my own abilities, and they have helped out in many times of need. Finally, I want to thank my wife, Chen, who has patiently waited for me to finish school. Without her help I could not have worked so hard for so long.

TABLE OF CONTENTS

LIST OF TABLES

LIST OF ILLUSTRATIONS AND CHARTS, ETC

LIST OF ABBREVIATIONS

- TRITC, tetramethylrhodamine isothiocyanate
- FITC, fluorescein isothiocyanate
- E-Box, CACGTG sequence
- T-Box, T-domain, Brachyury recognition sequence
- MLP, adenovirus MLP promoter
- LCR, human β-globin locus control region
- Myn4, Max protein without the N terminus 1-21 aa sequences
- bHLH, basic/helix-loop-helix
- IPTG, isopropyl-β-D-thiogalactopyranoside
- Max, Myc-associated factor X
- Mad, MAX dimerization protein
- Mxi1, MAX-interacting protein 1
- MNT, a novel Max-interacting protein
- Mlx, Max-like protein x
- USF, upstream stimulatory factor

INTRODUCTION

Chapter 1. The Myc/Max/Mad network: components and structure

c-Myc originally got its name for the ability to cause *my*elo*cy*tomatosis in susceptible animals and cultured cells (40). The Myc gene is well known as an oncogene and overexpression of Myc protein or Myc gene exists in a wide variety of human cancer cells (5,22,23,25,37,38). It is now well established that the deregulated expression of c-Myc plays a significant role in human cancer development. The Myc proteins, including C-Myc, N-Myc, and L-Myc were all indicated as direct regulators of gene expression (5,23,26,31). Thus C-Myc, N-Myc, and L-Myc have different transcriptional activities (6,23,27,31,40,57). They have similar protein secondary structure, bHLHZ (basic-helix-loop-helix-leucine zipper) domain. Also, to establish their transcription activities, the Myc families specifically bind the DNA sequence CACGTG (E-box) when dimerized with Max protein, a small 103aa bHLHZ protein which is consistently expressed in vivo (16,58). The crystal structure of Myc-Max (Figure1) was determined and suggests that a head to tail pair of Myc-Max dimers may, in turn, form a heterotetramer capable of bridging distant E-boxes (60).

The basic-helix-loop-helix-zipper (bHLH-Zip) motif of those proteins is a conserved region of approximately 70 amino acids shown to be responsible for protein dimerization. The conserved basic region at the N-terminal side is believed to be required for DNA binding to the dimer (5). Another important region of this bHLH protein is the leucine zipper at the C-terminal end, which is necessary for high binding affinity and specificity of the protein for DNA and for dimerization stability (6).

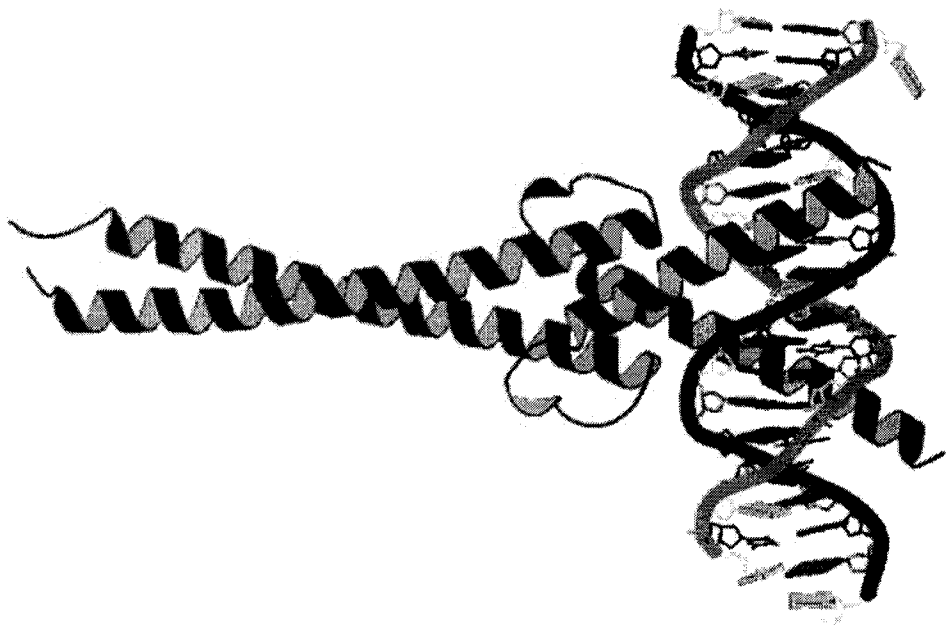

Figure 1. The structure of the Myc-Max heterodimer binding with 19-mer DNA oligos with E-Box sequence obtained from X-ray diffraction by S. K. Nair and S. K. Burley (60).

This crystal structure only contains the Max HLH domain (23-102) (80aa) and the c-Myc HLH domain (353-434) (82aa), with the binding of the DNA oligos 5'CGAGTAGCAC GTGCTACTC3' (sequence of complement chain not shown here), containing E-Box CACGTG sequence. The resolution was 1.80Å.

After the identification of Max as binding partner of different Myc proteins, including c-Myc, N-Myc, and L-Myc, there began a search for additional bHLHZip dimerization proteins. This search led to the discovery of the Mad (Max dimerization protein) proteins Mad1, Mxi1, Mad3, and Mad4, as interaction partners of Max, competing with Myc. Together these factors define the Myc/Max/Mad network (Figure 2) (34,40,81). Later two additional Max binding bHLH proteins, Mnt and Mga were found (42,43,45). Recently the identification of Mlx, a Max-like protein that can heterodimerize with Mad1, Mad4, and Mnt, but not with the other Mad proteins nor with Myc or Max, has been reported (12,59). The most recent extensions of the network are the cloning of MondoA as an Mlx binding partner (11) and the identification of WBSCR14, a transcription factor expressed from exon of Williams Beuren syndrome chromosome region 14, which also interacts with Mlx (19). Both Max and Mlx proteins are the central components of the network (Figure 2). Thus it is possible that not all members of this network have been discovered yet and it will be of interest to identify additional components that may further expand the network laterally and increase the whole complexity.

Comparing the structure of the different network components reveals similarities but also differences (Figure2). As expected from the identification of these factors as dimerization partners, all components possess a bHLHZip motif as a required interface for DNA binding/dimerization. Max as well as Mlx is capable of forming homodimers, which the other components could not. All these dimers function as DNA binding competent complexes that recognize E-box DNA sequences and have been suggested to function at

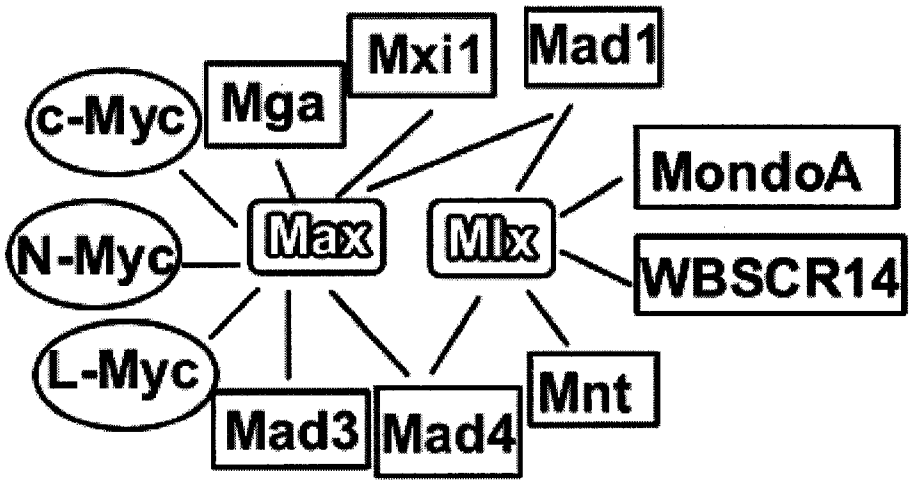

Figure 2. The complicated network of Myc/Max/Mad

The components of the Myc/Max/Mad network are indicated. Lines linked between each component define the known interactions between different network members. The interactions are specified by the BHLHZip dimerization domains. More detailed information about individual components is given in the text.

least in part as transcriptional regulators (24,34). The importance of the bHLHZip domains of both Myc and Mad proteins is supported by mutational analysis, demonstrating an essential role of this domain for all functions tested. Interestingly as far as analyzed, among all family members, only Myc, MondoA, and WBSCR14 proteins carry a transactivation domain (TAD) (Figure3), which may be related to their function of activating reporter genes through E-box elements (11,19,24). In contrast to Myc, Mad proteins and Mnt have an mSin3 interaction domain (SID), which mediates transcriptional repression. It was proved that besides bHLHZip, the SID is critical for the function of Mad proteins (49,51,72). Together these studies define the TAD of Myc proteins, the SID of Mad proteins, and the bHLHZip of all components as essential domains for the function of the respective network members. However detailed structure-function analyses of the proteins that have been identified more recently have not yet been performed. For instance, one of the proteins in the network, Mga, which is a very large protein of over 3000 amino acids. Its size distinguishes itself from the other members of the Myc/Max/Mad network, which in general are rather small molecules, and offers room for more structural domains which could be functional (Figure 3). Interestingly Mga carries two distinct DNA binding domains suggesting that it might regulate genes not only through E-box elements but also through sequences recognized by its T-box DNA binding motif (77). It is likely that further analysis of the different components of the network will reveal additional new and unexpected findings.

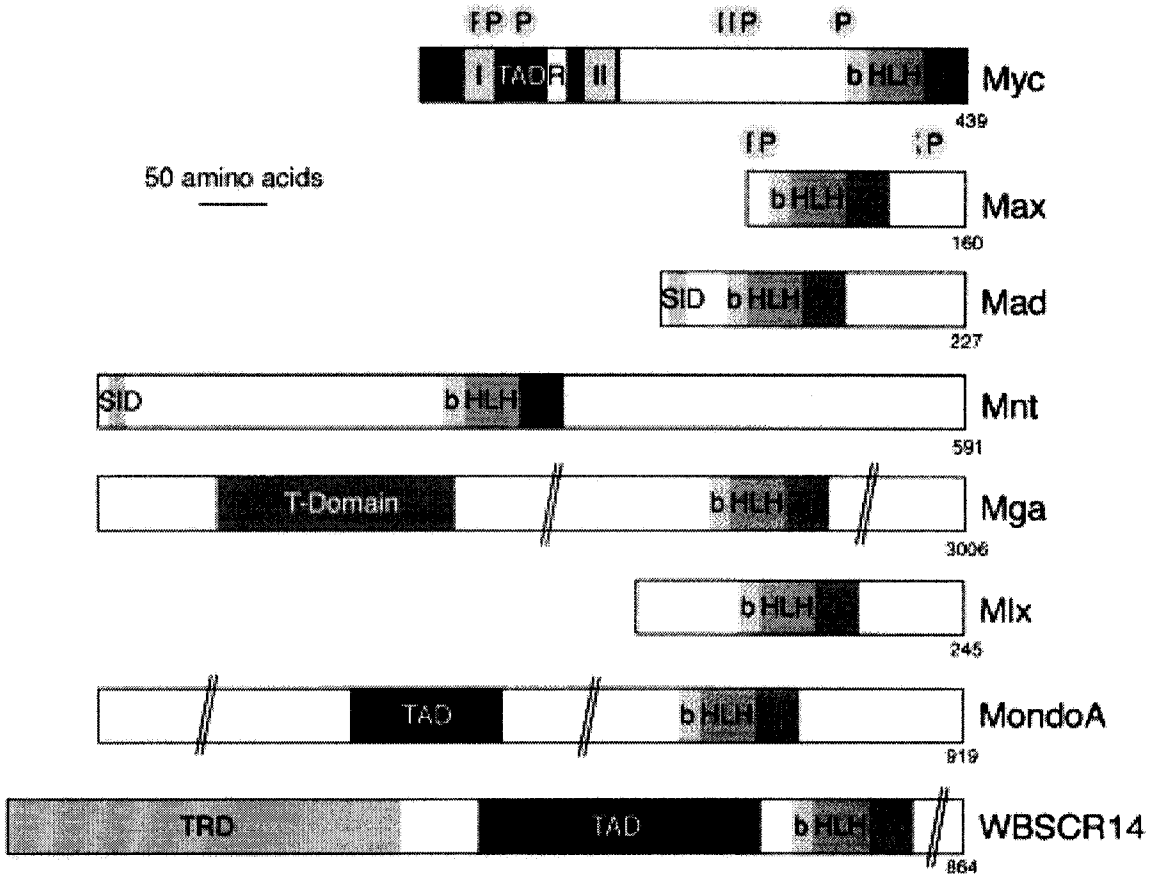

Figure 3. Structure-function schematic of components of the Myc/Max/Mad network. The proteins used in this study were Max (22-103, 10Kd). Myc (353-434, 10Kd) and Mad (1-220, 25Kd) (16,58).

The known functional domains of different network components are summarized. Information regarding the expression and the loss of function phenotypes, as far as defined, is indicated.

TAD: transactivation domain;
I: Myc box I;
II: Myc box II;
b: basic region;
R: region involved in repression;
HLH: helix-loop-helix domain;
Zip: leucine zipper domain;
SID: mSin3-interaction domain;
T-Domain: T-box DNA binding domain;
TRD: transrepression domain;
P: position of known phosphorylation sites.
The numbers refer to amino acids of the human proteins.

Chapter 2. The Myc–Mad antagonism: opposing functions on gene transcription regulation

After the identification of Mad1 protein (7,8), it was suggested that Myc/Max and Mad/Max complexes form a molecular switch involved in the regulation of transcription between different cell states. Myc/Max heterodimers are exchanged by antagonizing Mad/Max heterodimers on the responsive E-box elements on various genes (7,8). This model has been partially proved firstly from findings that Mad proteins inhibit reporter genes that are activated by Myc, interfere with transformation of rat embryo fibroblasts, block cell growth, inhibition of cell proliferation and prevent apoptosis (34,40,70). The findings were further supported by the analysis of Mad knockout and Mad transgenic mice, which provided the phenotypes originally expected (30,68,69). Further research found the overlapping and redundant roles of Mad proteins in different cell types. There are several Mad protein expressed in this HLH family, as a Mad family including Mad1, Mad3 and Mad4 (34,44). Other proteins in these families, such as Mnt and Mga, can also effectively compete with c-Myc, at least in vitro, which increased the complexity of this regulatory system. Those c-Myc antagonists are located in different types of cells. Mad1 and Mad4 are generally expressed in terminally differentiated cells, whereas Mxi1, Mad3, Mnt, and Mga, like all Myc genes, are also expressed in proliferating cells (41,43-45,67).

Generally, transcription factors regulate the transcription of specific genes at several different levels (33,76). It was suggested from the early findings that the transcription activators are important for the recruitment and activation of the polymerase complex.

Activators might also regulate the procession of the polymerase complex. In recent studies (53,79), it was shown that these activities are most likely downstream of effects on the chromatin structure of gene loci and more specifically of promoter regions. The structure of the chromatin appears to be the major determining factor in whether or not the promoter regions are accessible to the polymerase complex and thus the corresponding gene can be transcribed (53,79). Repression of transcription may also be initiated by affecting the polymerase complex but it is thought that the primary effects are on compacting chromatin and thus making it inaccessible for activators or the polymerase complex.

For the determination of chromatin structure, there were two fundamentally distinct mechanisms suggested. The first one involves the activity of molecules with ATPase and possibly helicase activity and then affects the structure and location of nucleosomes (32,50). The second mechanism targets histones, which involves different modifications on those proteins, such as phosphorylation, acetylation or methylation, leading to a multitude of differentially modified histones (21,75).. Different modifications on histones are thought to affect compaction of chromatin and to provide binding sites for other proteins. Some research has already shown that certain histone modifications have been linked to specific functional states of promoters (21,75).

For the transcription regulation mechanism of Myc/Max/Mad network, more recently evidence (16,58)was shown that the structural change of histones might be the primary determinant of transcription activation or repression. Binding of Myc induces cyclin D2

expression and histone acetylation at a single nucleosome in a MycBoxII/TRRAP-dependent manner(16). Thus the exchange from Myc/Max to Mad/Max complexes on *cyclin D2* is associated with recruitment of HDAC1, decrease in histone acetylation, and a loss of polymerase II binding to the *cyclin D2* promoter (16). This finding discussed above provides evidence for a possible mechanism, where each (HAT or HDAC) defines one consequence of the proposed switch, i.e. the alternate recruitment of HAT and HDAC activity to target genes (Figure 4). This suggests that the distinct regulation of histone acetylation in response to Myc/Max/Mad network members represent one level of the functional antagonism of Myc and Mad proteins. Currently there is little evidence for additional Mad-interacting proteins that are involved in the regulation of gene transcription. Several other factors implicated in the regulation of transcription have been identified that bind to Myc, such as INI1/hSNF5, a component of the multiprotein SWI/SNF complex, interacting with the C-terminal domain of Myc that is involved in an ATP-dependent chromatin remodeling pathway (20,50,64).

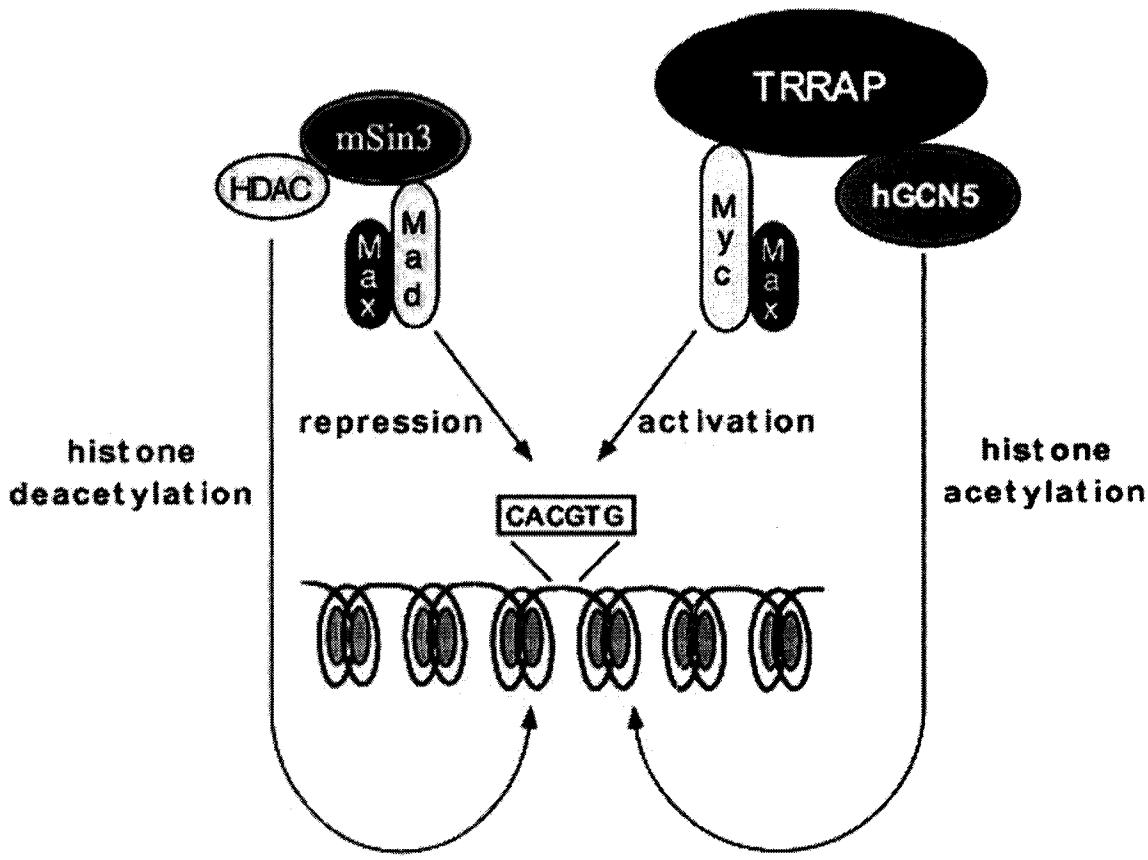

Figure 4. Model of the opposing biochemical functions of c-Myc and Mad suggest by S. B. McMahon, M. A Wood and M. D. Cole (58)

The demonstration here that c-Myc, through its essential cofactor TRRAP, recruits the HAT hGCN5 suggests a potential biochemical basis for antagonistic biological functions of c-Myc and Mad. In this model, c-Myc-Max heterodimers activate transcription of target genes by recruitment of TRRAP and a HAT such as hGCN5. HAT activity results in nucleosomal remodeling at target gene loci, allowing more efficient transcription. Following displacement of Myc-Max dimers from their cognate DNA recognition element, Mad-Max dimers recruit deacetylase activity to these sites, which in turn removes the acetyl groups from histones in nearby nucleosomes. This process facilitates chromatin condensation and consequently transcriptional repression.

The model of the switch from Myc-activating to Mad/Mnt-repressing complexes discussed above is simple enough. But since Mad protein families, and Mnt and Mga, all can effectively compete with c-Myc for binding to Max, it seems that it is simply a question of levels. One could expect that the sum of the levels of these antagonists should far exceed the level of Myc. If these complexes share the same targets, the equilibrium should always be in favor of transcriptional repression. Mad1 and Mad4 are generally expressed in terminally differentiated cells, whereas Mxi1, Mad3, Mnt, and Mga, like all Myc genes, are also expressed in proliferating cells (41,43-45,67,81). These findings have proposed a hypothesis that these proteins form a network centered around Max, whereby Myc activity is regulated by competition for Max by Mad or Mnt. Why so many antagonists would exist to regulate Myc functions is still unclear.

In addition, the simple model of the Myc-Max-Mad network is that Mad functions antagonize those of Myc by competing for Max (34), but recently, two additional Mad-specific interacting proteins have been discovered. First, Mad-member-interacting protein 1 (Mmip-1), a protein that contains a RING finger (a specialized type of Zn-finger consisting of 40 to 60 residues that binds two atoms of zinc) and a Zip domain, dimerized with the Zip domains of all Mad family members but not with those of c-Myc or Max, and this interaction blocks Mad's suppressive effects on Myc functions (36). Mmip-2, yet another RING finger protein, also blocks Mad functions through interactions with the Mad Zip domain and, when overexpressed, can sequester Mad1 into the cytoplasm (80). The problem for the Mmip-1 and Mmip-2 studies is that their interactions with Mad have been shown only in over expression experiments, which is a common problem to many studies in the field. However, if these interactions are physiological, the function of Mad-

Max complexes can be inactivated by interactions of Mad with Mmips. The net result of this scenario is that more Max would be available to bind to Myc.

Chapter 3. Central role of Max in Myc/Max/Mad Network in the interaction with DNA

The Myc-Max-Mad network model proposed by Eisenman and his colleagues long ago point out the central role on Max protein (8), which activate transcription when associated with Myc but repress transcription when bound to Mads or Mnt. This model implies that Myc-Max, Max-Max, and Mad/Mnt-Max complexes exist in equilibrium and the shift in this equilibrium decides whether or not transcription of target genes containing CACGTG elements are activated or repressed (Figure 5) (34).

Myc's ability to promote growth and transformation has been suggested to be opposed by a number of Myc antagonists. The most important findings of this research field were from Blackwood and Eisenman (14) and others (65) that Myc's ability to bind to its cognate DNA recognition E-box site (CACGTG), activate transcription, and promote cell proliferation, transformation, or apoptosis requires its dimerization with another bHLHZip binding partner Max (1-4,13,15,65). Unlike that of Myc genes, Max constitutively exists in cells (10), and this small protein is stable with a respectively longer half-time (47,65). Max, but not Myc, is also capable of undergoing homodimeration *in vitro*, and at least exists in nuclear extracts *in vivo* (56), thus the role that Max homodimer may play remains unclear (9,36,54,65).

Current research has shown Myc's regulation of various cellular processes to be a function of its interactions with a wide range of molecules (71). Several Myc-interacting proteins bind to Myc through HLHZip interactions that are also required for binding to

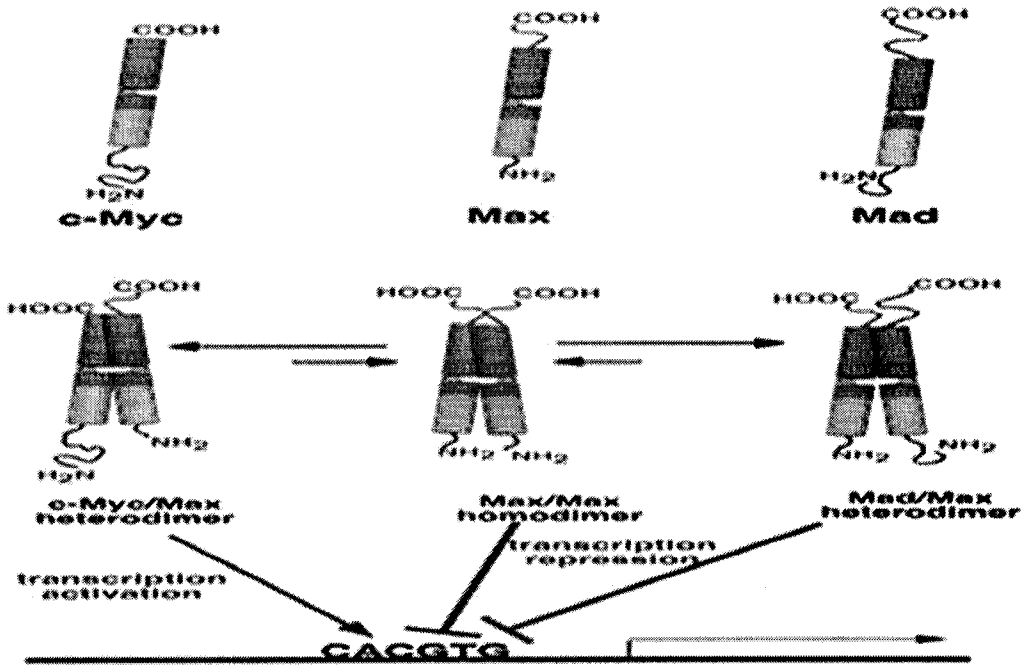

Figure 5. Diagram of the binding model of Max homodimer, Max/c-Myc heterodimer or Max/Mad heterodimer with DNA CACGTG element.

This model implies that Myc-Max, Max-Max, and Mad/Mnt-Max complexes exist in equilibrium and that shifts in this equilibrium dictate whether transcription of target genes containing CACGTG elements is activated or repressed

Max (71). Although, it is not saying that all of the Myc functions can be attributed to its dimerization with Max. For the precise contributions of other Myc partners, further studies are needed. Indeed, Max makes a critical role in this scenario, as its deletion, like that of Myc, compromises cell growth. This is not so for the other factors that have been proposed to regulate Myc activity by interacting with Max. In particular, the deletion of three of the Mad family members has essentially no impact on development; cell growth, survival, and differentiation; or tumor susceptibility. Thus, it remains to be determined whether Mad, Mnt, Mga, and possibly other yet unidentified factors play an important physiological role in regulating Myc activity.

In principal, signaling that regulates protein-protein interactions, and/or DNA-binding or transcriptional activity will affect the balance of Myc-Max versus Mad/Mnt-Max complexes. For example, *in vitro* experiments, phosphorylation of serines 2 and 11 of Max by casein kinase II impairs the DNA binding of Max-Max complexes (9,10). and the phosphorylation of c-Myc by different kinases has been implicated in regulating its transcriptional activity (35,39,61,66). Finally, the model implies that all of the dimer complexes in the Myc-Mad-Max network compete for common DNA target sites, E-Box (34). However, Myc-Max heterodimers bind only a subset of the sites bound by Max homodimers, due to a differential recognition of the flanking sequences (13,48,63,74), and different residues within the bHLH region of Mad family members have been suggested to play a role in the recognition of different E-box sites (63). Furthermore, Myc has also been shown to bind to noncanonical (non-E-box) sites (13). Thus, although this model has been useful for understanding the opposing effects of Mads, Mnt, or Mga on

targets that are activated by c-Myc, the details are still unclear.

In conclusion, it is difficult to fit all of the available data into a simple linear Myc-Max-Mad network. It is better to consider all data with the concept of a network, in which several parallel yet cross-linked pathways are involved in decisions that regulate the cellular behavior. Max certainly plays a central role in this network by targeting multiple transcription factors.

Chapter 4. Experimental approaches to the interaction between DNA and Max/Myc/Mad network

There have been a voluminous number of studies done on the Max/Myc/Mad network. But most of the work was focused on the biological function of this system, specifically the transcriptional regulatory functions which relate to descriptive and qualitative data.. There have been very little quantitative data on the interaction between the protein families and DNA. An understanding of how these proteins interact with DNA is a first step in understanding the mechanism of action of this important biological process. Our work was aimed to precisely measure the binding affinity of each interacting step. The result will help us to understand the complexity of the Max/Myc/Mad network interactions and their relationship.

This dissertation project was conceived out of the need to fill an apparent void that seemed to exist in the understanding of the complexity of the interactions of the herein discussed transcriptional factors. The approach was taken to measure the binding affinity of each interaction step. The questions that we want to answer for this transcriptional factor system include some of the following:

- What is the binding affinity of Max, Max-c-Myc and Max-Mad to DNA oligomers containing the E box and to other oligomers with various base substitutions? Quantitative data need to be retrieved to show and compare the binding affinity of interactions with different permutations.

- What is the specificity on the recognition of the E-Box (CACGTG sequence) element of Max-c-Myc, Max-Mad heterodimers compared with the Max homodimer?
- What is the appropriate interaction pathway of Max/Myc/Mad protein dimerization and protein-DNA interaction?
- What are the energy contributions of the protein-protein interaction and Protein-DNA interactions, specifically the entropy and enthalpy change in the binding process?
- Is there a preferential orientation of the protein dimer on the DNA binding site?

The methods used here to quantitatively measure the binding of a series of combinations of Max and other transcriptional factors on DNA is fluorescence polarization. Fluorescence resonance energy transferring (FRET) was used to analysis the orientation of protein on the DNA binding site. The details of experiments are in the following chapters. The model of interaction pathway of Max/Myc/Mad protein dimerization and protein-DNA interaction is diagrammed in Figure 6, where two binding models are suggested.

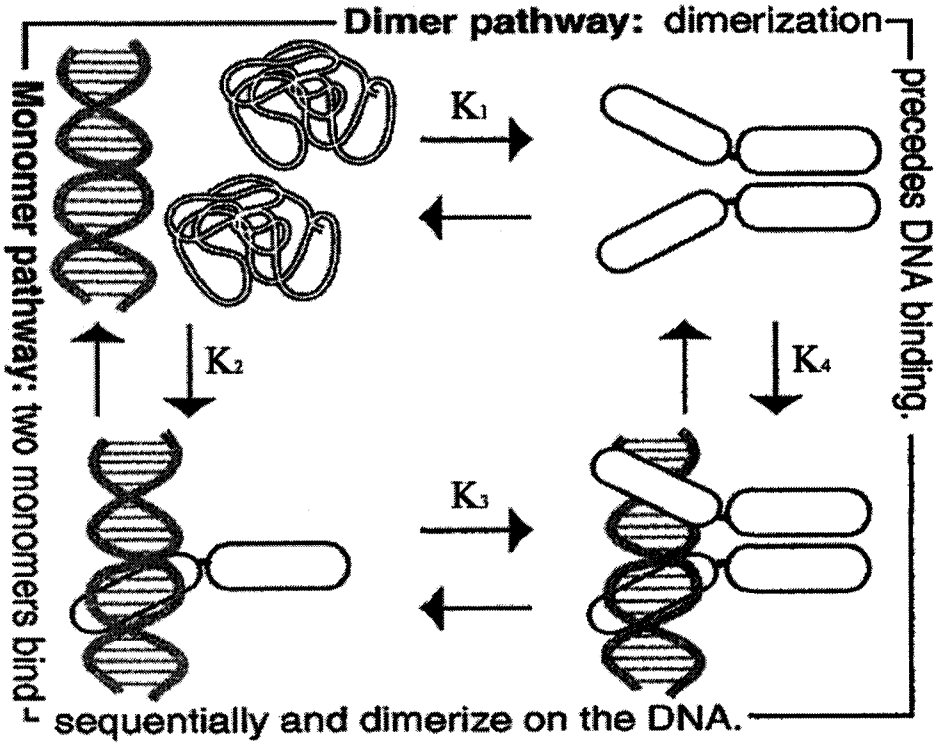

Figure 6. Dimer pathway or Monomer pathway: two models for the sequence of protein dimerization and DNA interaction in Myc/Max/Mad network. The diagram was modified based on some previous research on Jun/Fos interaction (52).

Two models are suggested here for the sequences of protein dimerization and DNA interaction with Myc/Max/Mad network. In one pathway, the Max monomer binds with the DNA first, then the second monomer (Max, c-Myc or Mad) joins in to form that dimer-DNA complex, thus in another pathway, protein dimerization occurs first, then dimer binds to the DNA.

MATERIALS AND METHODS

Chapter 1. Preparation and purification of Max, c-Myc and Mad Protein

In order to acquire sufficient proteins, genetically engineered bacterial hosts were constructed by transforming the hosts with expression vectors. Thus under certain induced conditions, these bacterial clones were induced to express the proteins of interest in large quantities for these studies. The proteins used in this study were Max (22-103, 10Kd), Myc (353-434, 10Kd) and Mad (1-220, 25Kd).

1. The construction of Expression Vectors of Max, Mad1 and c-Myc

The expression vectors Max/pET3a and c-Myc/pGex3T-2 were obtained from Dr. S. K. Burley's Lab in Rockefeller University. Several other constructions for Max, c-Myc have been tried with series of different plasmids to find the constructed vector with highest protein expression yield, but the expression of Max or c-Myc did not work as efficiently as the original hosts. The expression vector Mad1/pET30a was constructed using the strategy shown in Figure 7.

The detailed protocols are as following:

The 20μL pET30a vector and 20μL Mad cDNA PCR product were digested by adding 1μL of restriction enzyme EcoRI and HindIII for 3 hours in 37°C. 2μL reaction mix was taken out to run the Agarose gel to check the efficiency of the digestion

↓

The digested pET30a plasmid was purified by using the QIAquick® spin column (protocol in Appendix 3.1)

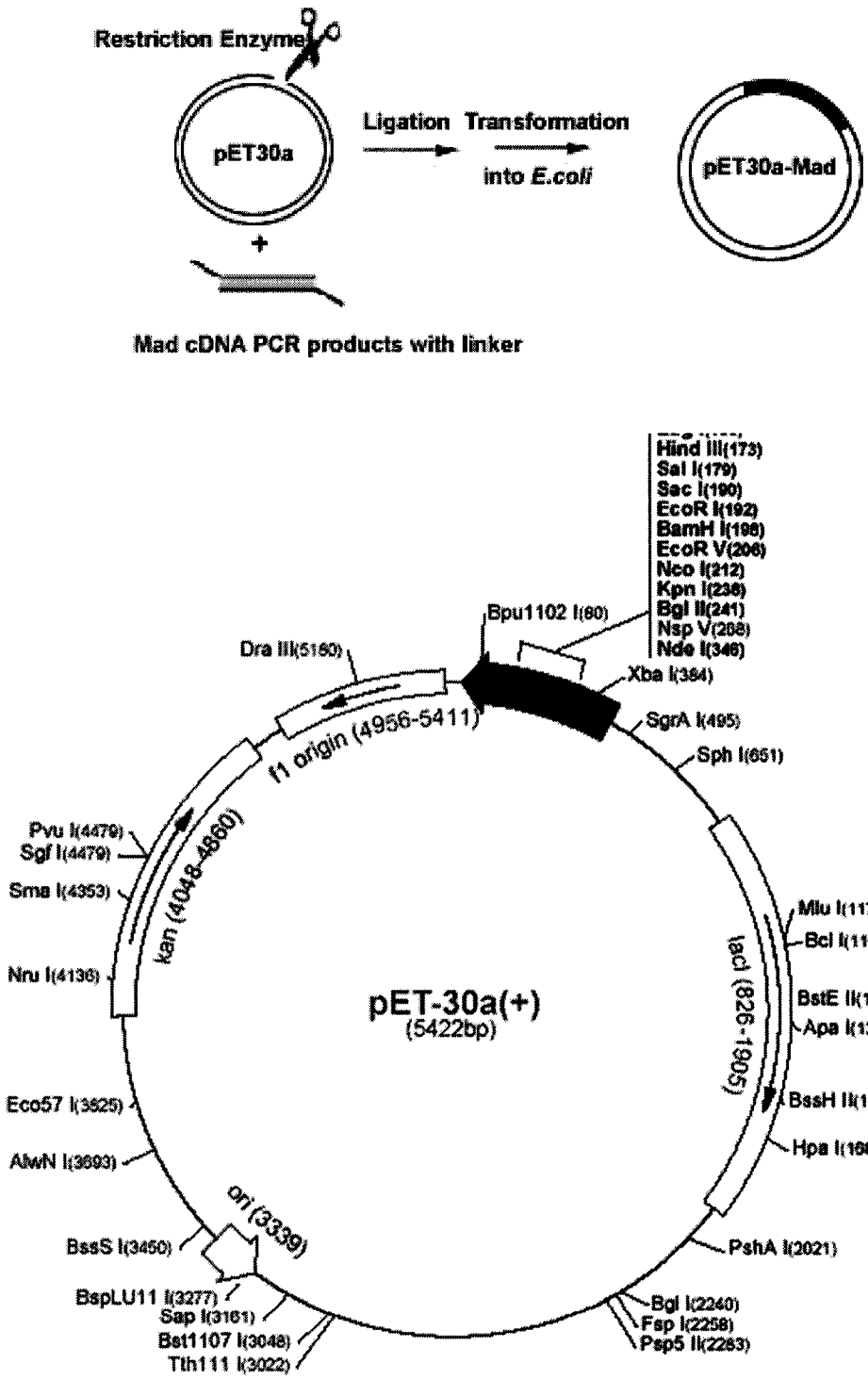

Figure 7. DNA cloning using Mad cDNAs as PCR products

↓

The digested cDNA PCR product was purified by using the QIAquick® PCR purification column (protocol in Appendix 3.2)

↓

Ligation reaction was performed at room temperature, using Novagen® Clonables 2X Ligation Premix (protocol in Appendix 3.4)

↓

1μL of ligation product was transformed to 50μL BL21plys competent cell (Purchased from Novagen®) on ice

↓

After 60-second 42°C heat shock, the competent cell was incubated with 300μL SOC media (Appendix 1.1) in 37°C for 1 hr

↓

Plate 100μL of it on the Kanamicin contained 2% agar plates for 18hrs incubation in 37°C, till the colonies on the plates were shown very clearly.

The cDNA sequences of all three proteins were obtained by using the online searching engine on Entrez-nucleotide dialog boxes at:

http://www.ncbi.nlm.nih.gov/entrez/query.fcgi?db=Nucleotide

The keywords used for the searching were human Max protein cDNA, human c-Myc protein cDNA and human Mad protein cDNA.

PCR primers were designed by using Primer3 online program for all three cDNAs corresponded to the 3' and 5' sequences of cDNAs as shown in table 1:

Table1. cDNA sequences of Max, Mad and c-Myc proteins

Protein Name	3' and 5' sequences of cDNAs
Max	5'ATGAGCGATAACGATGAC.....AGAAGCTCCGGATGGAGGCCAG CTAA3'
Mad	5'ATGGCGGCGGCGGTTCGGAT.....GTCACAAGGCGTGTCTTGGTC TCTAA3'
c-Myc	5'ATGCCCCTCAACGTTAGCTT.....TACGGAACTCTTGTGCGTAA3'

And the sequences of designed primers are listed in the following:

Table 2. The sequences of the PCR primers for Max, Mad and c-Myc cDNAs.

Protein	Primer Name	Primer Sequences	Tm	Annealing* temperature
Max	Max5'	5'TAAA*GGATCC*ATGAGCGATAACGAT GACATCG3'	55°C	52°C
	Max3'	5'TATA*CTCGAG*TTAGCTGGCCTCCATC CG3'	56°C	
Mad	Mad5'	5'AAAT*GAATTC*ATGGCGGCGGCGGTT3'	59°C	56°C
	Mad3'	5'CCC*AAGCTT*GAGACCAAGACACGCCT TGTGAC3'	60°C	
C-Myc	C-Myc5'	5'CGC*GGATCC*ATGCCCCTCAACGTTAG CTTCACC3'	61°C	56°C
	C-Myc3'	5'CCC*AAGCTT*AGAGTCTCTGCTGGTGG TGGG3'	60°C	

* Tm is calculated by using the online calculator in www.e-oligos.com, restriction enzyme site in Italic.

The cDNA amplification was done by PCR. The components of the PCR reaction mixtures in this experiment are:

3'Primer (50pmol/μL)	1μL
5'Primer (50pmol/μL)	1μL
cDNA template (100ng/μL)	0.5μL
2xPCR Mix for Promega	25μL
Nuclease Free Water	22.5μL
Total Volume	50μL

The PCR reaction was performed on PTC-100 PCR Mini-cycler by following protocol:

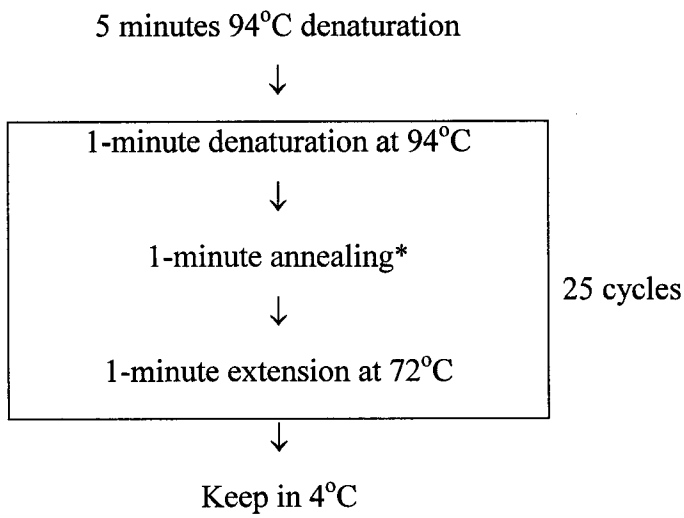

The PCR (polymerase chain reaction) products were purified by QIAquick® PCR Purification Kit (protocol in Appendix 3.2) and then were identified by 0.8% Agarose Gel electrophoresis and stained by Ethidium Bromide (Detailed protocol on Appendix 3.3). The electrophoresis result was visualized under UV illuminators.

A second PCR experiment was then performed to determination the success of tranformation and ligation products. The components of the PCR mix were the same as the first PCR except for the absence of cDNA template. Aliquot 25μL of this PCR mix into a PCR tube for each colony to be picked. Pick colony with a 10μl pipette tip. Dab the pipette tip into the master mix then place the tip in a correspondingly labeled culture tube. Run PCR reaction in 95°C (1mins) - 56°C (1mins) - 72°C (1mins) for 25 cycles, making sure to begin the PCR protocol with a 5-minute extended time at 95°C. Run 10μL of the PCR reaction on an Agarose gel to identify which cultures to keep for plasmid DNA isolation.

The small-scale expression of those vectors was done prior to the purification of proteins by detecting the protein expression level from SDS PAGE (protocol in Appendix 2.3), and comparing the density of the corresponded bands on the gel with the standard protein marker. It was found that the best expression vectors for these three proteins are pET3a/Max, pGET-2T/c-Myc and pET30a/Mad.

The pET30a plasmid used for the expression vector construction was purchased from EMD Biosciences.

2. Protein Expression and purification through classic chromatography and affinity chromatography

The Max, Mad and c-Myc protein were all expressed in BL21-pLys cell. The detailed protocol was as follows:

E.coli cells with expression vectors were incubated in 10ml LB media with 50ug/ml ampicillin (or 50ug/ml Kanamicin for Mad) at 37°C overnight

↓

This 10ml was transferred into1-litre LB media with 50ug/ml ampicillin (or 50ug/ml Kanamicin for Mad) for 3hrs at 37°C until the OD_{600} went up to about 0.6

↓

4ml 100mM IPTG solution was added into the LB as the induction reagent and the cell was incubated for 6hrs at room temperature

↓

The pellet was collected after 20-minute centrifugation in 6000 rpm and the net weight of pellet was measured

↓

The pellet was resuspended in 2xpellet weight (ml) HEPES buffer (pH7.6) (see Appendix 1.2) on ice with protease inhibitor cocktail (Appendix 1.2) and about 0.1mg lysozyme for 1 hour

↓

The cells were broken with 3 times 30-second sonication on ice. The supernatant was collected after 30 minutes centrifugation in 18000rpm

For Mad and c-Myc, the remained pellets were also saved for treatment of inclusion bodies. Because of the formation of inclusion bodies in the expression of Mad and c-Myc protein, the following protocols were used to unfold and refold the target proteins:

The pellet (inclusion bodies) was washed twice with 10ml HEPES buffer (pH7.6) containing 1% triton X100

↓

The pellets were collected after spinning at 18000 rpm for 30min at 4°C

↓

The pellets (inclusion bodies) were then solubilized in 2 ml 50mM HEPES buffer pH7.6, 6M guanidine HCl, 25mM DTT and left for 1h on ice

↓

Insoluble material was removed by centrifugation at 18000rpm for 30 minutes at 4°C

↓

The saved supernatant was diluted as quickly as possible into 20ml cold (4°C) 50mM HEPES pH7.6

Max protein was purified by using a salt concentration gradient elution on Hitrap® SP ionic exchange chromatography, following the same protocol described before(29,73)(also see Appendix 2.1). Mad protein was purified on Ni^{2+}-His Trap affinity column (Sepharose resin was purchased from Novagen) (Appendix 2.2). GST fused c-Myc protein was purified on GST affinity column (From Amshan-Phamacia). The protocols of purification through affinity chromatography followed the company product technical manual(62) (also see Appendix 2.3). Purified proteins were dialysized against 50mM HEPES, pH7.5 and concentrated with centricon® YM4000.

3. N-terminus labeling Max protein with tetramethylrhodamine-5-isothiocyanate (5-TRITC)

The Max protein primary amine on the N-terminus was labeled by TRITC in the following reaction:

Max protein concentration was adjusted to ~ 1.0 mg/ml in 50mM HEPES buffer (pH7.6) and total volume of the protein was about 5.0ml

↓

TRITC was dissolved in anhydrous DMSO and the concentration was determined as 1.5mg/ml. 100 μl TRITC was added per 1 ml of protein solution

↓

The protein-dye mixture was incubated overnight in the dark at 4 °C with continuous gentle agitation.

↓

Labeled protein was separated from free Rhodamine compounds by eluting from 30ml Sephedex G15 gel filtration column with 50mM HEPES buffer (pH7.6). The first fraction was collected.

↓

The collected fractions were concentrated with centricon® YM4000 by centrifugation for 6 hours in 4000rpm

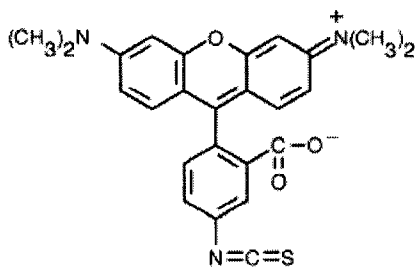

Structure of tetramethylrhodamine-5-isothiocyanate

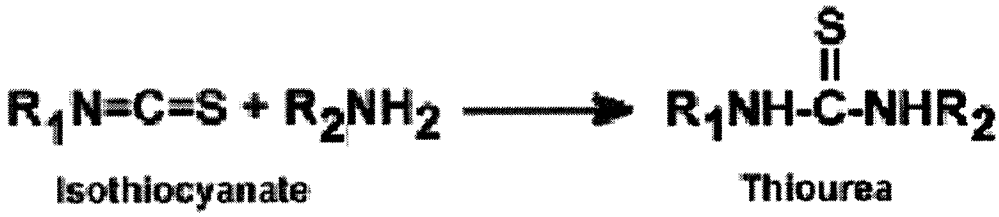

Figure 8. Reaction of a primary amine with an isothiocyanate.

The final protein concentration and F/P ratio was determined by measuring absorbance at 280 nm and at 555 nm. The following formula was used to obtain approximate values:

Firstly $A_{protein} = A_{280} - A_{555} \times (CF)^*$

$CF = (A_{280\ free\ dye})/(A_{555\ free\ dye}) = 0.30$ for TRITC

So, the protein concentration is:

$[Protein] = A_{protein}/1.4$ (mg/ml)

$F/P\ ratio = (MW \times A_{555}) / [Protein] \times \varepsilon$

Here ε=93000 for TRITC

Buffers containing TRIS are not acceptable since amine groups on TRIS interfere with labeling, the buffer used here was HEPES, pH 7.6.

Chapter 2. Preparation of DNA Oligonucleotides

The DNA oligomers used were also synthesized with fluorescein labeling at the 5' end to measure equilibria for fluorescein-labeled DNA-Max/Myc/Mad interactions. The DNA oligomers were 21-, 16- or 12-mers in length and are based on the adenovirus MLP promoter containing the E-box. Sequences with 3 bases that are different from the MLP sequence is based on the human globin locus control region (LCR) transcription complex which contains the USF binding site (18). A modified LCR (mLCR) sequence with three other different mutations and a base mismatch in the E-box were also used as a protein-binding target. Three 21-mer oligos were used to measure the ΔG difference for variations in the E-box sequence. For the FRET experiment, the 21-mer E-Box oligos with FITC (emission at 513nm) labeled on either ends were used as the energy donor in the energy transfer measurement with TRITC (excitation at 575nm) on Max protein N-terminus as the acceptor. All oligos as well as PCR primers for the protein expression vector construction were purchased and synthesized from Gene Link.

All sequences of oligos are listed below:

E-box: underlined,

Mutant bases: shown in italic and bold

Complementary strand not shown:

Table 3. The designed DNA oligos for the experiment interacting with proteins

Oligos	DNA sequences (complementary strand not shown)
12-mer MLP	5'GGCCACGTGACC3'
16-mer MLP	5'TAGGCCACGTGACCGG3'
16-mer LCR	5'TAG***A***CCAC***C***TGAC***T***GG3'
16-mer mLCR	5'TAGGCCAC***C***TG***C***C***TC***G3'
21-mer E-Box	5'GTGTAGGCCACGTGACCGGGT3'
21-mer Half-Ebox	5'GTGTAGGCCA***G***GTGACCGGGT3'
21-mer Non-Ebox	5'GTGTAGGCCA***GC***TGACCGGGT3'

Chapter 3. Fluorescence Anisotropy Measurements

As shown in Figure 9, an electron at ground state is excited by photons from external source such as a lamp or laser to excitation singlet state S_1' (stage1). After decay (stage 2), the energy of S_1' is partially dissipated to a lower vibrational energy state S_1 and then it returns to its ground state by emission (stage 3). Once the energy is released as photons in this three-stage process at a certain energy state, it is termed "fluorescence".

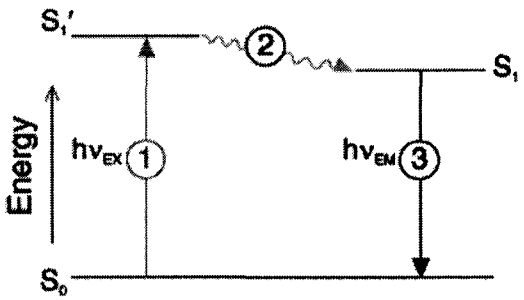

Figure 9: Scheme of basic theory of fluorescence (from www.probe.com)

The fluorescence measurement can be limited to only certain directions by measuring the polarized fluorescence signal change. (As shown in Figure 10). Anisotropy is used to calculate the polarization. The anisotropy of fluorescence (A) is determined from the equation:

$$A=\frac{(I_{\parallel} - I_{\perp})}{(I_{\parallel} + 2I_{\perp})}$$

Where $I_{//}$ and $I_{\perp}$ are the parallel and perpendicular fluorescence emission intensities, respectively. Anisotropy measurements are based on the average angular displacement that a fluorophore undergoes from the absorption to the emission of the photons. The change in the anisotropy will be observed when there is a change in the environment, such as a ligand binding to the fluorescent molecule, which will cause a reorientation of the fluorophore.

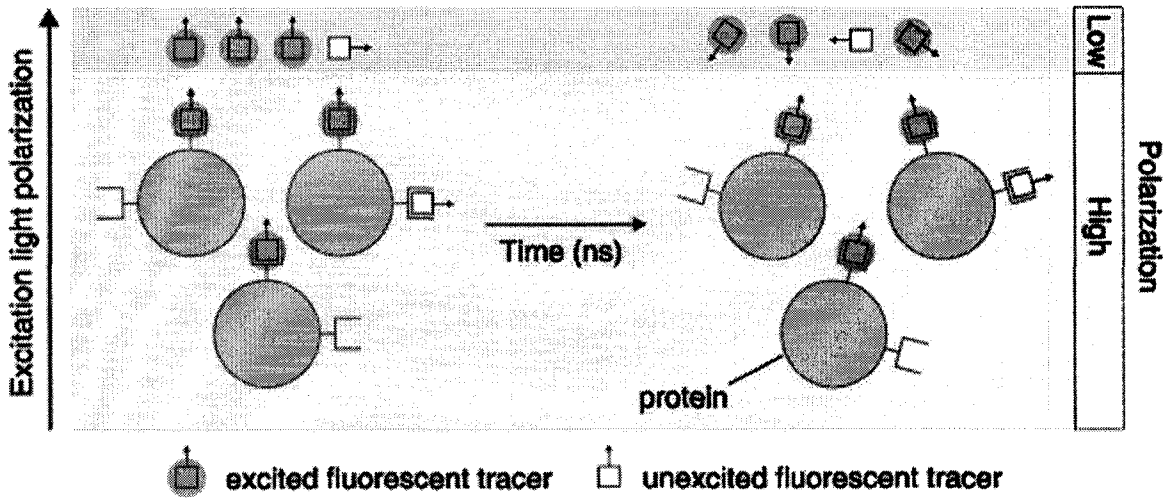

Figure 10: Physical basis of fluorescence polarization assays. Dye molecules with their absorption transition vectors (arrows) aligned parallel to the electric vector of linearly polarized excitation light (along the vertical page axis) are selectively excited. For dyes attached to small, rapidly rotating molecules, the faster rotations prior to emission, resulting in low fluorescence polarization. Thus, binding of the low molecular weight tracer to a large, slowly rotating molecule like protein results in high fluorescence polarization. Fluorescence polarization therefore provides a direct readout of the extent of tracer binding to proteins, nucleic acids and other biopolymers.(From www.probe.com)

Chapter 4. Titration

All fluorescence measurements were carried out on a SPEX Fluorolog τ2 spectrophotometer. The signal pathway used was L-format. The slides on the excitation path and emission path were all set to 6 mm. For the temperature dependence experiment, the cuvette chamber was connected with the water bath. Temperatures were monitored with a cuvette attached micro probe, which was connected to the Fisher 202 thermometer (error below ±0.5°C).

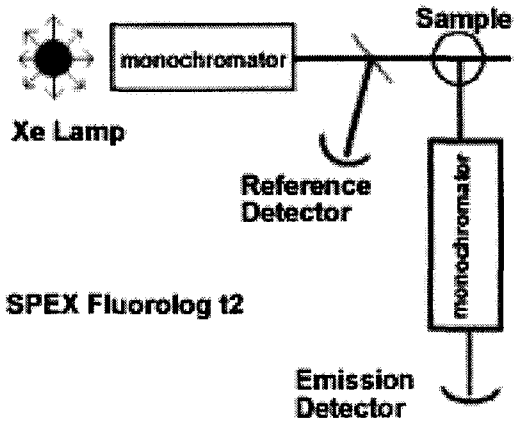

Figure 11. Scheme of Spex Fluorolog in L-format

RESULTS

The protein-protein and protein-DNA binding equilibria were measured by monitoring the fluorescence anisotropy of the labeled Max and labeled DNA oligonucleotides. In the experiments, when the Max protein was added to the solution with labeled DNA, Max protein interacted with the fluorescent DNA molecules and caused an anisotropy change. In our experiments, we measured the increase in the anisotropy signals of the labeled DNA or labeled Max upon addition of the corresponding ligand.

For the simple binding reaction where competitive interaction is not observed and thus one can obtain the theoretical equation for the K_d (dissociation constant) between Protein-protein and Protein-DNA with following:

For a simple binding reaction $A + B \Leftrightarrow C$

The dissociation constant, K_d, is defined as*:

$$K_d = \frac{[A][B]}{[C]}$$

Here, $[A] = [A]_t - [C]$

$$[B] = [B]_t - [C]$$

$$\text{So, } K_d = \frac{([A]_t - [C])([B]_t - [C])}{[C]}$$

$$[C]^2 - ([A]_t + [B]_t + K_d)[C] + [A]_t[B]_t = 0$$

Solving this equation results in:

$$[C] = \frac{\left[([A]_t + [B]_t + K_d) + \sqrt{([A]_t + [B]_t + K_d)^2 + 4[A]_t[B]_t}\right]}{2}$$

Since the normalized anisotropy change $\Delta r = \frac{(r - r_0)}{(r_\infty - r_0)} = \frac{[C]}{[A]_t}$, the [C] in the above solution is replaced by $\Delta r \times [A]_t$

Therefore,

$$\Delta r = \frac{\left[([A]_t + [B]_t + K_d) + \sqrt{([A]_t + [B]_t + K_d)^2 + 4[A]_t[B]_t}\right][A]_t}{2}$$

*The definitions of symbols in the equations:
[A]: concentration of chemical A at equilibrium
[B]: concentration of chemical B at equilibrium
[C]: concentration of chemical C at equilibrium
$[A]_t$: totaling concentration of chemical A
$[B]_t$: totaling concentration of chemical B
r_0 : initial anisotropy signal
r: anisotropy signal in each titrations
r_∞: the maximum anisotropy signal (saturation state)

In the expression above, Δr and $[B]_t$ are two variables with two parameters, $[A]_t$ and K_d. By inputting and running this equation in KaleidaGraph™ data analysis program, the dissociation constant for each interaction can be obtained. The data were fit to a single equilibrium constant K_d. More details of data fitting are also described elsewhere (78). The designed DNA oligos for the experiment interacting with proteins are listed as following:

Oligos	DNA sequences (complementary strand not shown)
12-mer MLP	5'GGCCACGTGACC3'
16-mer MLP	5'TAGGCCACGTGACCGG3'
16-mer LCR	5'TAG***A***CCAC***C***TGAC***T***GG3'
16-mer mLCR	5'TAGGCCAC***C***TG***C***C***TC***G3'
21-mer E-Box	5'GTGTAGGCCACGTGACCGGGT3'
21-mer Half-Ebox	5'GTGTAGGCCA***G***GTGACCGGGT3'
21-mer Non-Ebox	5'GTGTAGGCCA***GC***TGACCGGGT3'

Before the titration, 50μL of each of two DNA complementary oligonucleotides were mixed in 1.5 ml Eppendorf tubes. The oligonucleotides mixture was denatured by incubating at 70°C heating block for 30 minutes, and then annealed at room temperature for 1 hour before being placed on ice. The oligonucleotides mixture was diluted to 20μM. The purified Max, c-Myc, and Mad proteins were all concentrated and the concentration determined by the Bradford method (17) (Appendix 2.4). The Max protein concentration is based on the assumption that the Max protein (20μM) is a dimer under high concentrations. Max/c-Myc and Max/Mad heterodimers were prepared by mixing 1-fold Max protein with 2-fold c-Myc or Mad 24 hours before the titration experiment. The final concentrations of Max, Max/c-Myc and Max/Mad protein were ~20μM.

The binding experiments were performed in 25 mM HEPES-KOH, pH 7.6 buffer containing 50 mM KCl, 10 mM DTT, 5 mM $MgCl_2$, 0.5 mM EDTA. The total volume of buffer in Helma™ 1ml quartz cuvette was set to 400μL. 1μL labeled oligonucleotide or Max protein was added to the cuvette to a final concentration of 50nM. The titration was performed by transferring and mixing the binding ligand into the cuvette and detecting the anisotropy signal collected by the spectrophotomer emission detector and generated in the DataMax2.0 program. The overall titration volume increase was not over 20μL, which minimized the systematical error below 5% due to dilution.

Figure 12. MLP DNA oligonucleotide (○) and LCR DNA oligonucleotide (●) titrated with Max Protein. The concentration of MLP was 20nM, LCR was 100nM. Anisotropy change was shown as Y value by increasing the Max protein concentration (X value). The titration curves indicate stronger binding affinity for MLP than LCR. The anisotropy signal was normalized by fitting the signal in saturation state as 1.0.

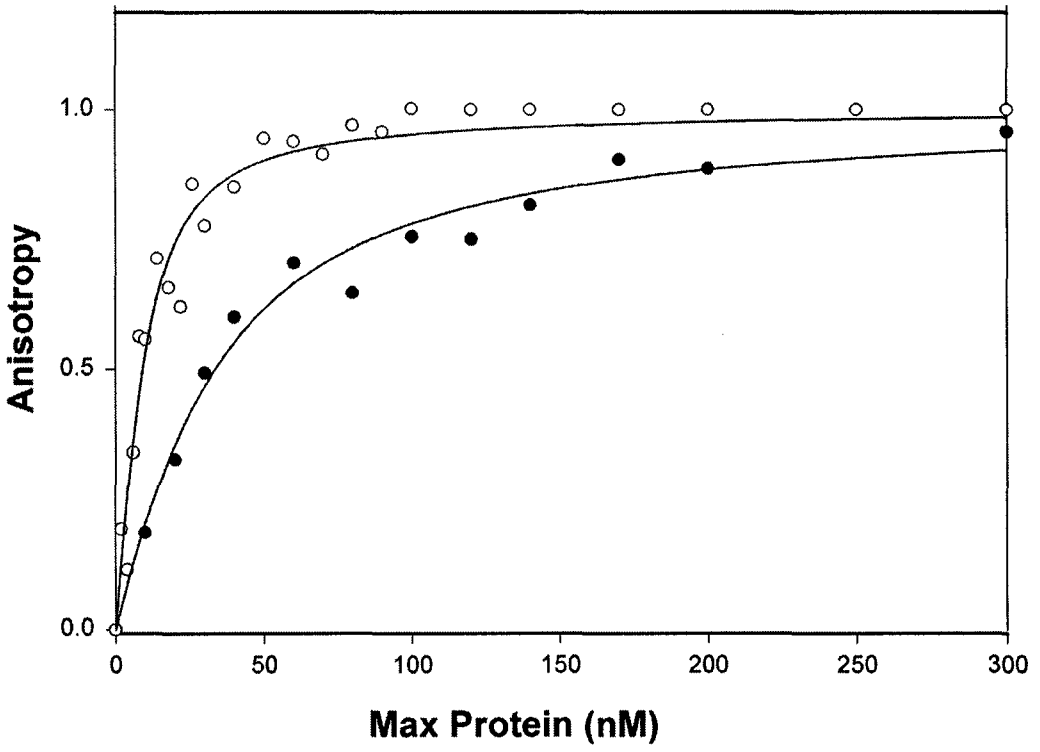

Table 4. Equilibrium binding and constants and specificities of USF and MAX with DNA

Oligos (12mers)	K_{eq} (nM) for USF[1]	Specificity	K_{eq} (nM) for MAX	Specificity
MLP	15±10	1090	2.2±0.5	104
LCR	3133±570	3.0	33.3±7.7	9.6
mLCR	9820±2680	1.0	230±10	1.0

1. Values from reference (73)

Chapter 1. Measurement of protein-DNA interaction

The titration data shown in Figure 12 demonstrate that there are significant differences in the binding affinity of Max protein to MLP and LCR DNA. The specific binding between MLP DNA and MAX is about 10-fold higher affinity than LCR DNA and about 100-fold tighter binding than for the mLCR sequence (Table 4). An interesting observation is that the final anisotropy of the bound DNA is considerably higher for the MLP DNA than for mLCR or LCR DNA. This suggests that the binding mode may lock the DNA into a more rigid conformation for the specific binding, allowing less rotation even at the terminus where the fluorescent label is attached. This could be accomplished by interactions outside the E-box binding region such as a hydrogen bond between an amino acid in the loop region of the protein and the flanking sequence of the DNA. It is also possible that there could be a charge interaction between an amino acid side chain such as Lys 57 and a residue in the flanking sequence. We have determined the pH dependence of the binding between pH 6.5 and 8.5 (data not shown). No significant changes in binding affinity as a function of pH were found. This would indicate that if a charge residue is involved, it does not have a pK near this pH range.

It has been shown that the Max dimer has two binding sites in one E-box; one for each monomer (29). The series of oligonucleotides described in Materials and Materials as E-box, Half-Ebox and Non-Ebox were constructed to examine the contribution of each half of the E-box to Max binding affinity and stability. These oligonucleotides also allow us to assess whether or not there is cooperativity between the two half-sites. The

cooperativity between these two sites can be determined by the free energy differences in binding. At equilibrium, the free energy change for specific binding is given by:

$\Delta G^{o}_{E\text{-}Box} = -RTlnK_1$

$\Delta G^{o}_{Half\ E\text{-}Box} = -RTlnK_2$

$\Delta G^{o}_{Non\ E\text{-}Box} = -RTlnK_3$

Consider binding by each half-site and determine cooperativity:

$\Delta G^{o}_{Non\ E\text{-}Box} = -RTlnK_3 = 2\Delta G^{o}_{Non\ specific}$ (For each half site) (1)

$\Delta G^{o}_{Half\ E\text{-}Box} = -RTlnK_2 = \Delta G^{o}_{E\text{-}site} + 2\Delta G^{o}_{Non\ specific}$ (2)

Where $\Delta G^{o}_{E\text{-}site}$ is the additional free energy due to the specific site.

$\Delta G^{o}_{E\text{-}Box} = -RTlnK_1 = 2\Delta G^{o}_{Non\ specific} + 2\Delta G^{o}_{E\text{-}site}$ (3)

We can now determine two $\Delta\Delta G^{o}$ functions:

$\Delta\Delta G^{o}_{3,2} = (3) - (2)$ and $\Delta\Delta G^{o}_{2,1} = (2) - (1)$

This $\Delta\Delta G^{o}$ represents the additional free energy for the specific site (1/2 E Box)

To the extent that these 2 numbers are different, indicates cooperativity, non-cooperative or anti-cooperative binding. The binding curves are shown as Figure 13. A comparison of the equilibrium values in Table 5 shows that for Max homodimer, $\Delta\Delta G^{o}_{3,2}$ = 2.2kJ and $\Delta\Delta G^{o}_{2,1}$ = 3.1kJ. There is an 0.9 KJ/mol ΔG^{o} difference between these two numbers, showing there is a slight cooperativity in the Max binding with DNA to the two sites. Thus binding to one site slightly stabilizes the second binding site.

Figure 13. Anisotropy of interaction between Max protein and 3 different oligos

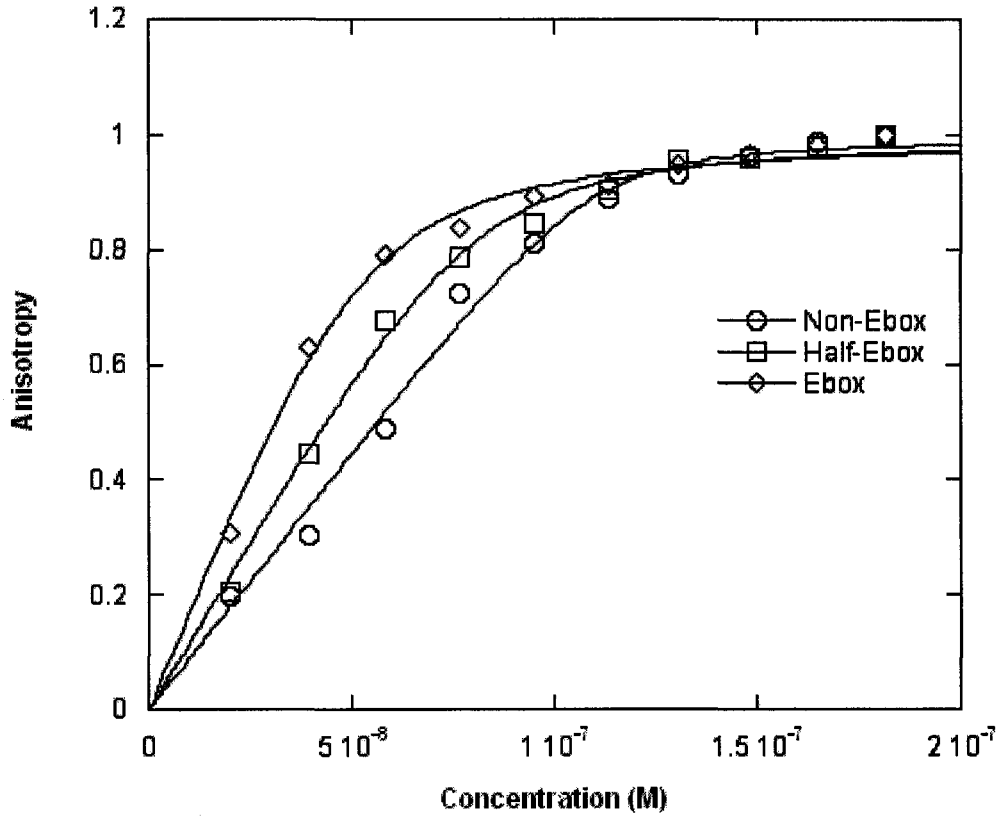

Table 5 Dissociation Constants (K_d) and ΔG for the Max protein binding with different oligonucleotides with Ebox, Half-Ebox and Non-Ebox sequences. All constants are in nM.

Oligos (21mers)	Max_2 K_d (nM)	ΔG^o(kJ)	Max-c-Myc K_d (nM)	ΔG^o (kJ)	Max-Mad K_d (nM)	ΔG^o (kJ)
Ebox	19.2±4.4	43.3±0.5	90.5±25.4	39.6±0.8	192±48	37.7±0.6
Half-Ebox	48.7±8.3	41.1±0.3	229±35	37.3±0.3	315±83	36.5±0.6
Non-Ebox	170±15	38.0±0.2	-------	------	-------	------

The same titration experiment has been performed with Max-c-Myc and Max-Mad heterodimer to detect the free energy contribution of their interactions which the same DNA sequences with which Max homodimers interact. The results showed the similarity between the two heterodimers, but they were very different from the Max homodimer (Table 5). For the heterodimers, the binding affinity with E-Box is 4 timer weaker than the Max homodimer for Max-Myc heterodimer but 10 times weaker for Mad-Max. The free energy difference between non-specific binding and E-Box binding were much larger then the Max homodimer with DNA, even the heterodimers showed no binding ability to the non-Ebox sequences. (Table 5).

To determine the related thermodynamic constants for different interactions, the van't Hoff equation relates the equilibrium constant to temperature and allows us to extract Δ H and Δ S for the interaction:

$$\Delta G^{o} = -RT \ln K_{eq} = \Delta H^{o} - T\Delta S^{o}$$

Rearrange to:

$$lnK_{eq} = -\frac{\Delta H^{o}}{RT} + \frac{\Delta S^{o}}{R}$$

A plot of $\ln K_{eq}$ vs. 1/T yields a straight line with slope = $-\Delta H^{o}/R$. This type of plot is called a van't Hoff plot. Here it is assumed that the enthalpy change is independent of temperature and the protein or DNA oligonucleotides are stable in the higher temperatures.

In titration experiments to detect the anisotropy change of different protein-DNA interactions, binding equilibria constants were determined for each interaction in three different temperatures: 10°C, 20°C and 30°C (Table 6). The data were plotted and analysized by KaleidaGraph™ (Figure 14). The entropy and enthalpy change were obtained from the plot fitting and the free energy change ΔG^{o} was then calculated for 20°C and physiological 37°C (Table 7).

Table 6. Binding constants (K_d) for DNA oligos interacting with Max-Max, Max-c-Myc and Max-Mad protein at various temperatures. All constants are in nM.

Temperature (K)	Max-Max	Max-c-Myc	Max-Mad
283.0	2.3±1.0	57±10	140±22
293.0	15.1±5.4	84±10	168±14
303.0	290±37	120±20	192±31

Figure 14. Van't Hoff plot for E-Box contained MLP oligos titrated with Max_2, Max-c-Myc and Max-Mad dimmers.

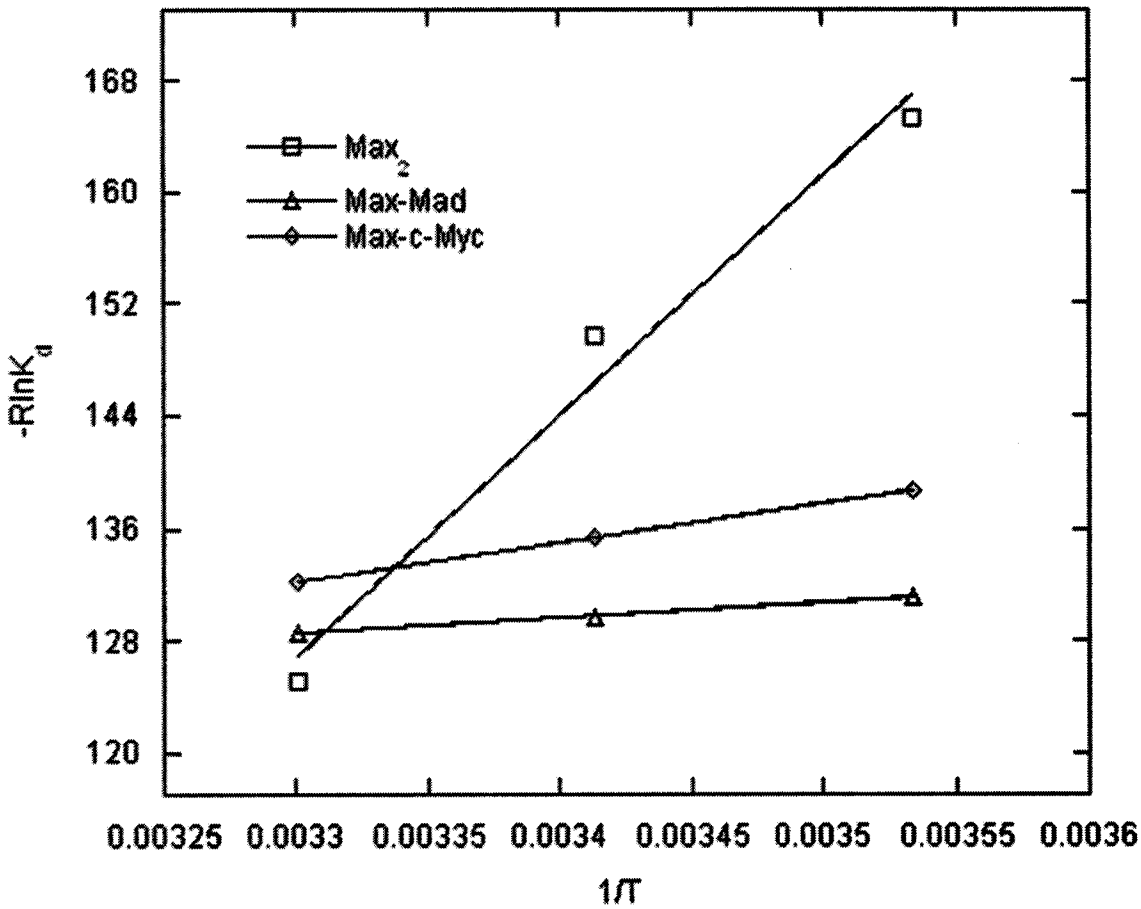

Table 7. ΔH^o, ΔS^o for MLP oligos binding with Max_2, Max-c-Myc, Max-Mad obtained from the van't Hoff plots

Protein	ΔH^o (kJ.mol^{-1})	ΔS^o (J.mol^{-1}.K^{-1})	ΔG^o(kJ.mol^{-1}) at 20°C	ΔG^o(kJ.mol^{-1}) at 37°C
c-Myc	-27.8±0.2	40.5±0.4	-39.7±0.2	-40.4±0.3
Mad	-10.9±0.1	93.0±0.9	-38.1±0.4	-39.7±0.3
Max	-171.5±3.5	-439.0±9	-42.8±6.6	-35.4±6.7

Chapter 2. Measurement of protein-protein interaction

The protein-protein interactions were measured by monitoring the fluorescence anisotropy of the TRITC labeled Max protein. In the experiments, when Mad, c-Myc or unlabeled Max protein were added to the solution with labeled Max, the dimerization of labeled Max with Mad, c-Myc or Max caused an anisotropy change.

Anisotropy could be used to compare the size of different molecules. Based on the Perrin relationship (55), the anisotropy displays a linear relationship to the rotational correlation time, θ. Since the correlation time is related to the hydrodynamic volume, the Perrin relationship can be written as the following equation:

r: anisotropy

$$\frac{1}{r} = \frac{1}{r_0} + \frac{\tau \cdot R \cdot T}{\eta \cdot V_h}$$

r_0: limiting anisotropy
τ: Lifetime
η: Viscosity
V_h: hydrodynamic volume

Where the correlation time, $\theta = \eta . V_h / RT$. In this experiment, if the fluorescent molecules with different hydrodynamic volumes coexist in a homogeneous solution, r, r_o and V in the Perrin equation will be replaced by the observed anisotropy, the mean limiting anisotropy of the molecules and the mean effective hydrodynamic volume of all fluorescent molecules in the solution, respectively. When the anisotropy increases to its saturation point, corresponding to the maximum ligands bound, the value of the anisotropy is proportional to the protein-DNA complex and the mean hydrodynamic volume V_h of the final Protein-DNA complex:

$$\frac{1}{r} \propto \frac{1}{V_h}$$

To compare the size of the Max/Max, c-Myc/Max, Mad/Max complex. Three protein samples: 20μM Max_2, 20μM Max-c-Myc, 20μM Mad-Max were titrated into TRITC labeled Max solution. TRITC labeled Max was added to 400μL HEPES buffer in the cuvette to a final concentration of 100nM. Three titrations were performed with those three different protein samples at room temperature (20°C). The titration results were plotted and fit by KaleidaGraph™ as shown in Figure 15. The difference on those anisotropy increases to saturation point reflect the difference on molecular size for these 3 complexes. The result showed that the Max-Max complex has similar size as Max-Myc complex, but the Max-Mad is much larger. In this titration system, the Max and c-Myc protein have the similar molecular weight about 10kD (for c-Myc, only bHLH domain got expressed), thus Mad protein has a molecular weight about 25kD. Once after the dimerization, the Mad-Max is about 2 fold larger than the Myc-Max, which caused the much higher anisotropy signal for Mad-Max interaction than Myc-Max did.

Figure 15. The anisotropy change for the TRITC labeled Max titrated with Max, c-Myc or Mad proteins.

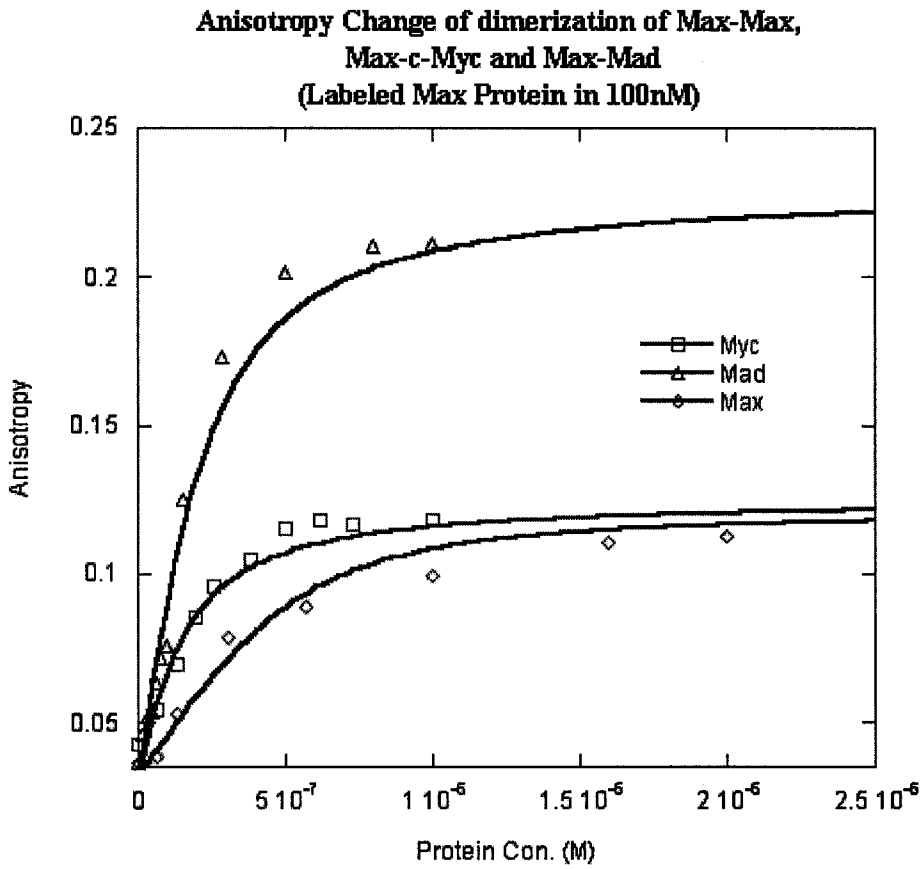

Van't Hoff plot was also used to analysis the interaction between the Protein-protein in various temperatures (Fig 16). Series of titrations on protein-protein interaction were performed in different temperatures and fitted data were listed in Table 8. The enthalpy and entropy of these interactions were determined from the temperature dependence (Table 9). Combined with the previous data (Table 7) of the Protein-DNA interaction, The overall ΔG^0 of this 2-step interaction for formation of the protein dimer-DNA complex was almost 4 KJ less favorable for Mad-Max-DNA formation at 20°C compared to Max_2-DNA or Myc-Max-DNA, which were essentially the same. However, at 37°C, Mad-Max-DNA and Myc-Max-DNA have essentially the same ΔG^0 while Max2-DNA was about 7 KJ less stable.

Table 8 Binding constants (K_d) for protein-protein interaction between Max-Max, Max-c-Myc and Max-Mad protein at various temperatures. Max was labeled with TRITC. All constants are in nM.

Temperature (K)	Max-Max (nM)	Max-c-Myc (nM)	Max-Mad (nM)
283.0	410±34	81.2±8.1	282±18
293.0	680±44	176±12	320±25
303.0	830±36	267±24	446±36

Figure 16. Van't Hoff plot for TRITC labeled Max protein titrated with Max, c-Myc and Mad proteins

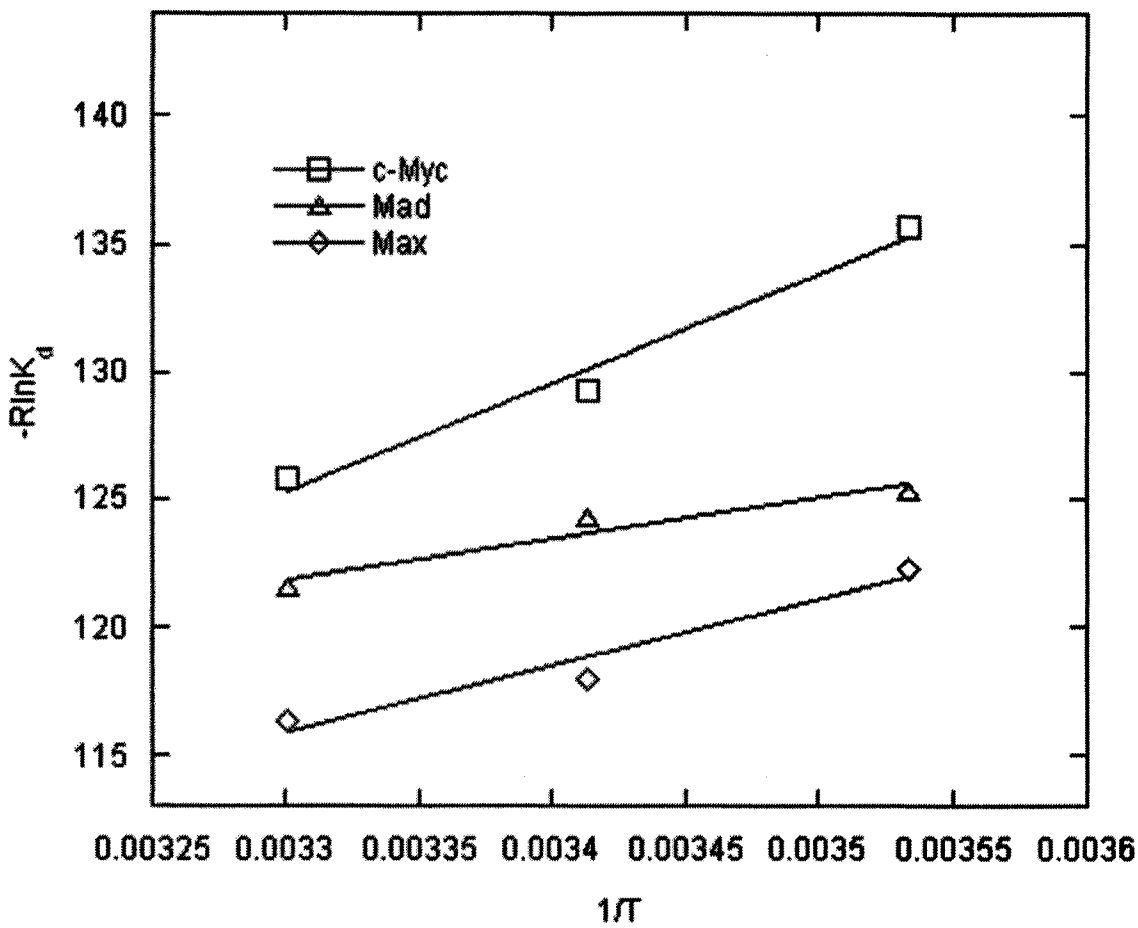

Table 9. ΔH^{o}, ΔS^{o} for Max binding with Max, c-Myc, Mad obtained from the van't Hoff plots

Protein	ΔH^{o} ($kJ.mol^{-1}$)	ΔS^{o}($J.mol^{-1}.K^{-1}$)	ΔG^{o}($kJ.mol^{-1}$) at 20°C	ΔG^{o}($kJ.mol^{-1}$) at 37°C
c-Myc	-42.6±0.5	-15.2±0.2	-38.1±0.6	-37.9±0.5
Mad	-16.3±0.6	68.0±2.5	-36.2±1.3	-37.4±1.3
Max	-25.7±0.6	30.9±0.7	-34.8±0.8	-35.3±0.8

Chapter 3. Measurement of interaction pathway of Max/Myc/Mad protein dimerization and protein-DNA interaction

As shown in Figure 6, two models are suggested here for the sequences of protein dimerization and DNA interaction with Myc/Max/Mad network. In one pathway, the Max monomer binds with the DNA first, then the second monomer (Max, c-Myc or Mad) joins in to form a dimer-DNA complex (monomer pathway), thus in another pathway, protein dimerization occurs first, then the dimer binds to the DNA (dimer pathway). In the experiments, Max protein and DNA Oligonucleotides were labeled with fluorescence probes. By detecting the anisotropy signal change due to the interaction, in each interaction step, the equilibrium constants K_1, K_2, K_3 and K_4 (Table 10) have been determined:

K_1, the dissociation constants of Max-Myc and Max-Mad dimerization, were determined by using the same titration methods for the measurement of protein-protein interaction described before.

K_3, the dissociation constants of Max-Myc dimer and Max-Mad dimer interacting with DNA, were determined by using the same titration methods for the measurement of protein-DNA interaction described before.

K_4, the dissociation constant of Max monomer-DNA complex interacting with c-Myc or Mad, were determined by titrating concentrated c-Myc or Mad protein (20uM) to TRITC labeled Max protein (50nM) and MLP oligo (100nM) mixture preincubated overnight. As shown in Figure 17, this binding between Max monomer-DNA complex with c-Myc protein was a thermodynamically very unfavorable step, which gave an about 15-fold and 25-fold larger dissociation constant value than K_1 and K_4.

Thus K_2, the equilibrium constants for Max monomer binding with E-Box, were calculated from K_1, K_3 and K_4. These equilibrium constants were obtained separately from two series of titrations with Mad or c-Myc protein, thus gave 2 values of K_2, 6.9nM and 10.3nM, showing a very tighter binding of Max monomer binding with DNA than the Max protein-protein dimerization.

Table 10. Equilibrium constants for the Protein-DNA interaction pathway indicated in Figure 6. K_1, K_2, K_3 and K_4 stand for the Equilibrium constants for each steps of the sequence of protein dimerization and DNA-Protein binding.

Protein	K_1 (nM)	K_4 (nM)	K_2 (nM)	K_3 (nM)
c-Myc	176±12	84±10	6.8±1.6	2200±100
Mad	320±25	168±14	10.2±1.8	5300±100

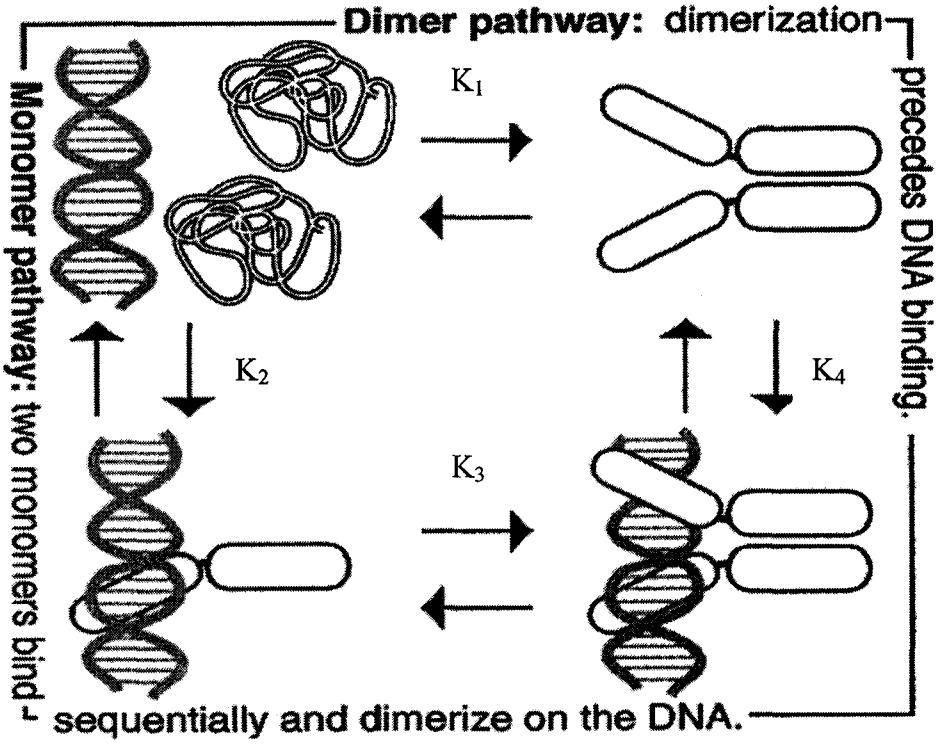

Fig 6. Dimer pathway or Monomer pathway: two models for the sequence of protein dimerization and DNA interaction in Myc/Max/Mad network. The diagram was modified based on some previous research on Jun/Fos interaction(52).

Figure 17. Anisotropy of interaction between Max monomer-DNA and c-Myc protein

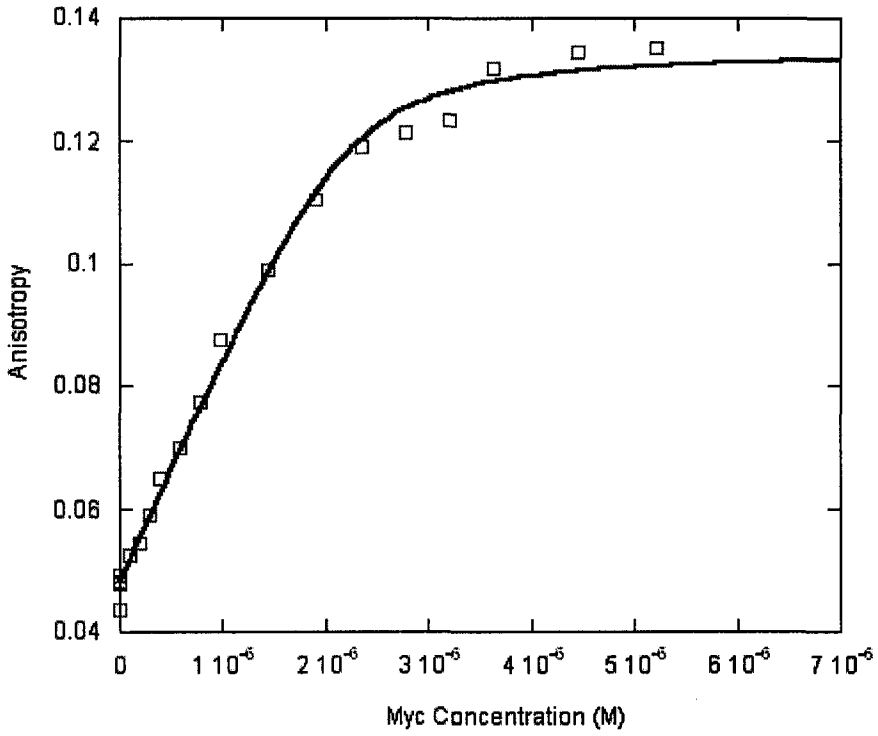

Chapter 4. Detection of preferential orientation of the Myc/Max/Mad protein dimer on the DNA binding site by Fluorescence Resonance Energy Transfer

Fluorescence Resonance Energy Transfer (FRET) is a distance-dependent excited state interaction in which emission of one fluorophore is coupled to the excitation of another.

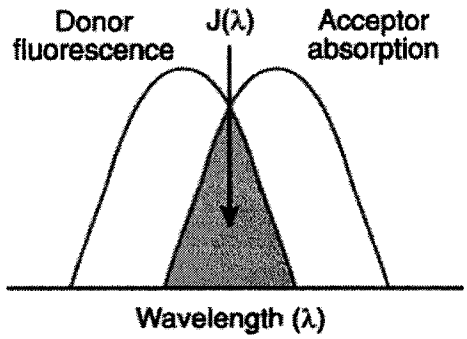

Figure 18. Scheme of Fluorescence Resonance Energy Transfer (FRET). Emission of Donor has an overlap with absorption of Acceptor. (From www.probe.com)

This interaction is due to the acceptor dipole interactions with the donor dipole. FRET can be used to obtain structural maps of complex biological structures, primarily proteins and other macromolecular assemblies such as ribosomes and nucleosomes. Currently, FRET has been used to study the orientation of DNA-binding proteins, such as Jun/Fos (52). Measurements of energy transfer can provide intra- or intermolecular distance data for proteins and their ligands in the range 10-100 Angstrom. Also, FRET can detect change in distance (1-2 Angstrom) between loci in proteins; hence it is a sensitive measure of conformational change. The excitation energy of donor probe can be transferred by a radiationless process to a neighboring fluorophore if their energy level difference corresponds to the quantum of excitation energy. The relationship between the transfer efficiency and the distance between the donor and acceptor, R is given by the equation:

$$E = \frac{R_o^6}{\left(R_o^6 + R^6\right)}$$

or

$$R = R_o\left(\frac{1}{E}\text{-}1\right)^{\frac{1}{6}}$$

where R_o is the Foerster distance, at which energy transfer is 50% efficient. At R_o, there is an equal probability for resonance energy transfer and the radiative emission of a photon. The magnitude of R_o is dependent of the spectral properties of the donor and acceptor:

$$R_o = \left(8.8 \times 1023 K^2 n\text{-}4 Q_d J\right)^{\frac{1}{6}} \text{(Angstrom)}$$

Where factors are defined as:

- K^2 or kappa square: dipole orientation factor, a function of donor emission transition moment and the acceptor absorption transition moment (range 0 to 4, generally $K^2 = 2/3$ is assumed)
- Q_d : fluorescence quantum yield of the donor in the absence of acceptor
- n: refractive index of the medium which is generally assumed to be 1.4 (range 1.33-1.6) for proteins.
- J: spectral overlap integral which represents the degree of overlap between the donor fluorescence spectrum and the acceptor absorption spectrum.

The donor and acceptor must be within 0.5 x Ro -1.5 x Ro from each other. These measurements give the average distance between the two fluorophores. When measuring a change in distance, the result is a scalar and gives no indication of which fluorophore (donor and/or acceptor) moves. From the crystal structure of Max-DNA complex, the

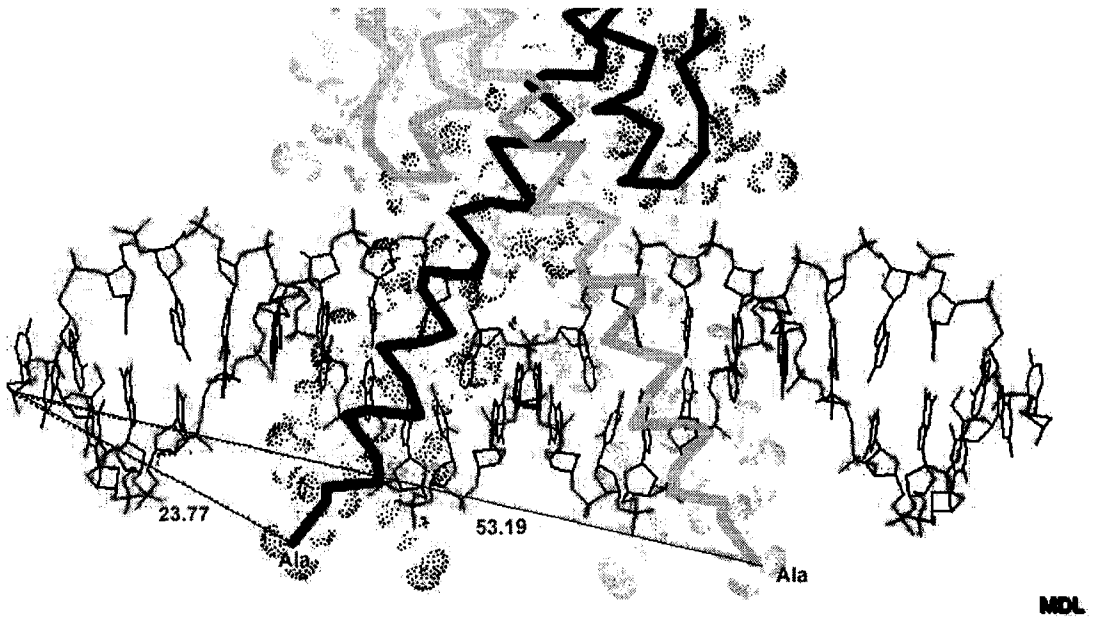

Figure 19. Crystal structure of Max_2-DNA 21-mer complex. The distances of Max N-terminus Ala12 to the 2 ends of the DNA oligonucleotides were indicated in above figure as 23.77Å and 53.19Å.

distance between N-terminus of Max protein to the 3' or 5' end of DNA oligos has been computed and shown in Figure 19. The length of designed oligonucleotides was 21 bases to fit the distance requirement for FRET.

To create FRET, a receptor, a donor and the distance between them are critical. In the experiment, the donor is FITC, which binds with the 3' or 5' of the DNA oligos, while the receptor is TRITC, which is labeled on the N-terminus of Max protein. Once the protein interacts with DNA, the receptor-donor coupling is formed to allow energy tranferring and FRET is detected by the FITC emission intensity decreasing as well as the TRITC emission intensity increasing (Figure 20). Since the Foerster distance Ro for FITC-TRITC coupling is 55 Å, respectively FRET would occur between these two fluorophores since the actual distance between the fluorophores is in 0.5 Ro to 1.5 Ro (27.5 Å to 73.5 Å) range.

The protein labeling procedures were described in the material and methods. The 5'and 3' FITC labeled 21-mer oligonucleotides and their complements were purchased from Gene Link. The TRITC labeled Max protein was incubated with c-Myc and Mad protein overnight in 4°C and final concentration of protein stock solution was determined as 50μM. In the titration, the DNA oligonucleotide was added into the cuvette in a constant concentration as 100nM. The protein was then titrated into the system. Data was collected with DataMAX program and analysized.

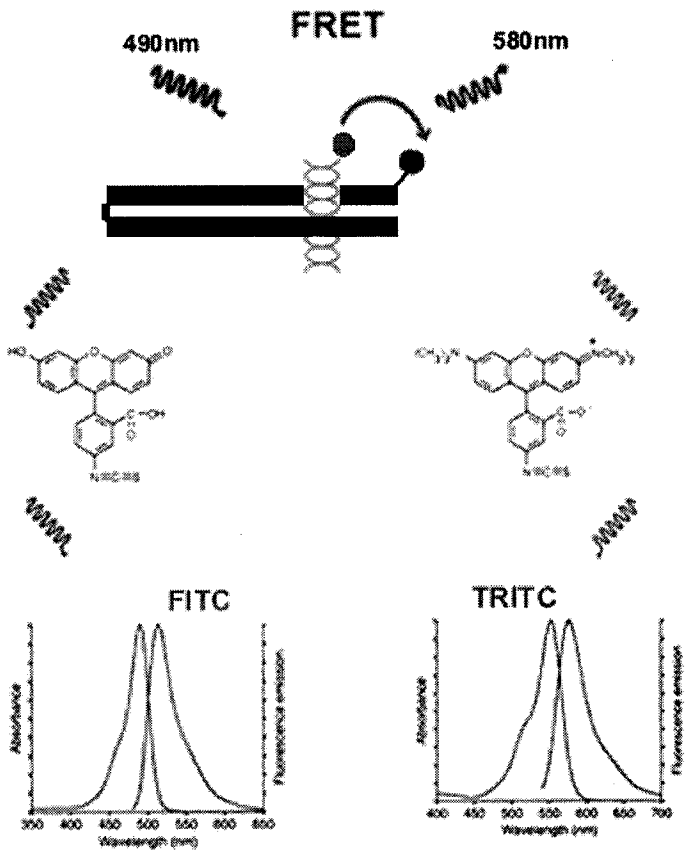

Figure 20. The scheme of FRET between Max protein (TRITC labeled) and DNA Oligos (FITC Labeled).

The FRET experiment was performed on the interaction between the Max_2, Max-c-Myc and Max-Mad with DNA oligos. The FITC was labeled on different ends of two 21 mer double strained DNA oligos with identical sequences. For the interaction between the homodimer and DNA, there was significant energy transferring to the TRITC on the Protein N-terminus from either oligos (Figure 21). Thus the protein had slightly higher energy transfer efficiency due to the shorter distance to the E-Box region from the 3' of this DNA oligo compare to 5' as expected. For the heterodimer interaction with DNA, the energy transfer efficiency was largely decreased in either Max-Myc or Max-Mad. But for the 3' labeled DNA or 5' labeled DNA, the energy transfer efficiency for each heterodimer showed no significant difference. These results suggest that there might not be an orientation difference for these two heterodimers anchoring on the E-Box.

Figure 21. FRET spectrum of Max_2, Max-c-Myc with FITC labeled 21-mer MLP DNA oligos

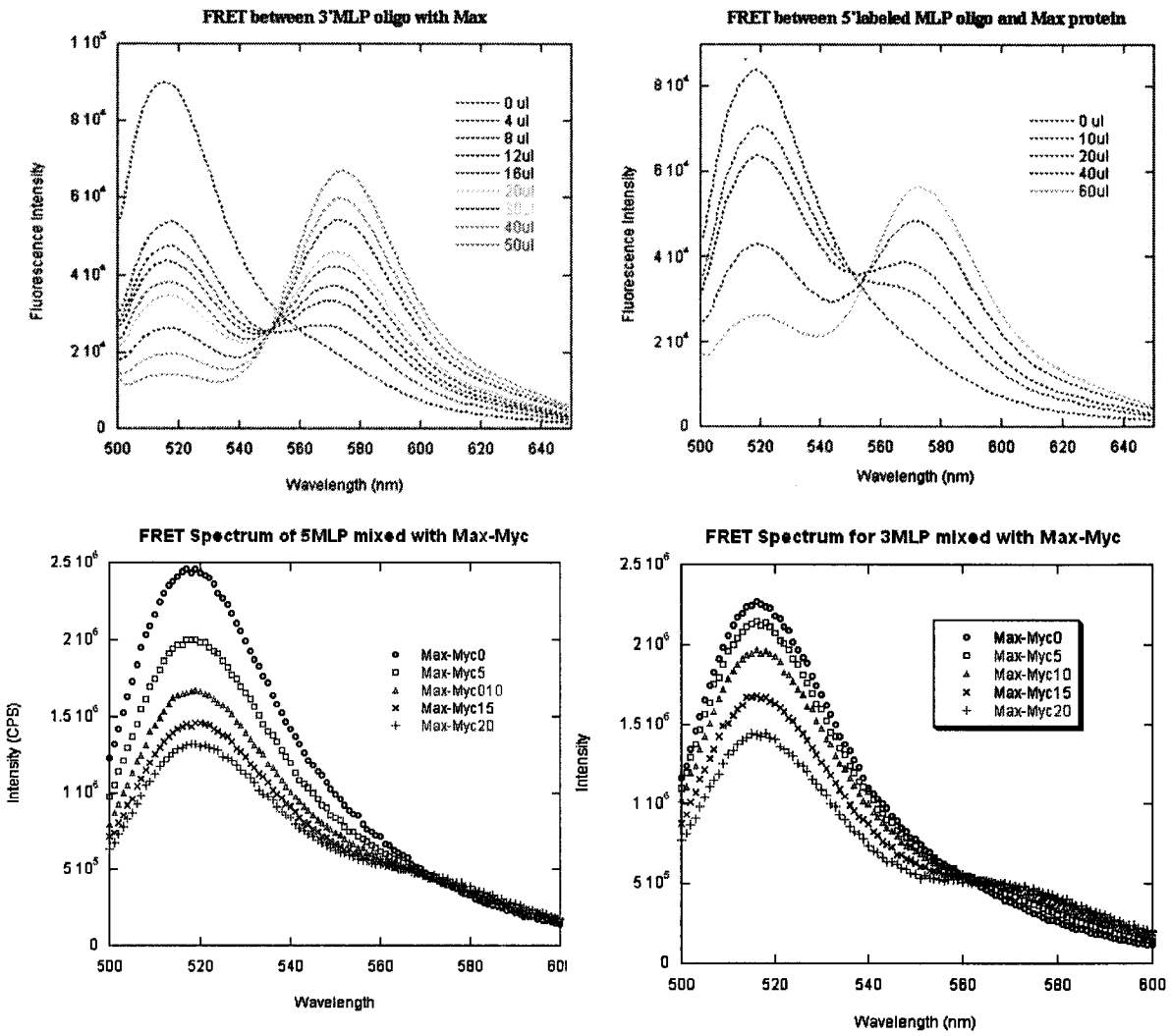

DISCUSSIONS

The data in Figure 12 (Page 41) show a single binding mode for Max binding to DNA. The Max-DNA binding profiles indicated Max dimer binding to DNA and did not show a biphasic binding mode which has been observed with USF (28,73). USF is another b/HLH/Z protein which recognizes the same E-box sequence and binds as two dimers (homotetramer) to two duplex DNA molecules (or to two E-box sites on the same DNA which forms a loop). A comparison of the binding constants (Table 4, Page 42) for Max and those of USF to MLP DNA shows that both bind with similar affinities (nM) but USF has 10 times higher specificity of binding to MLP DNA than Max. Max binds both LCR and mLCR DNA more tightly than USF. The lower specificity of binding of Max to MLP DNA suggests differences in transcriptional regulatory functions between Max and USF. USF is believed to mediate DNA looping by binding to two E-box sites in a biphasic mode--the first USF dimer binding tightly to one E-box and a second dimer binds with 10-fold lower affinity to the second E-box. The formation of a DNA loop is thought to be necessary for stimulating transcription and requires a high degree of specificity of USF for DNA. On the other hand, Max is known to activate transcription by binding to Myc oncoprotein and to cause repression of Myc transcriptional activities by forming heterodimers with Mad protein. Max function may be more important in determining the formation of heterodimers than in the selection of DNA.

The data (Table 5. Page 46) show that there is significant difference on the behavior of heterodimers interacting with DNA with the Max homodimer with DNA. Firstly, the Max protein is more functionally related to its high binding affinity to the DNA, thus the

recognition of DNA sequences is more likely contributed by Max's partner, Myc or Mad. These results also support some pervious studies on the binding preference that Myc-Max heterodimers binding only a subset of the sites bound by Max homodimer, due to a differential recognition of the DNA flanking sequences (8,36,80,81). The different residues within the bHLH region of Mad family members have been suggested to play a role in the recognition of different E-Box sites (14). Further more, Myc has also been shown to bind to noncanonical (non-E-Box) sites (65). Recent studies suggests that Myc and Mad, possesses identical DNA-binding specificities *in vitro* (46), which was supported by our data that Mad-Max and Myc-Max heterodimer behave similarly on the Half-Ebox and Non-Ebox oligonucleotides.

Secondly, the titration data (Table 7, Page 51) show that the binding affinity Max_2-DNA interaction was more affected by the temperature change than that of the heterodimer. It was shown from the Van't Hoff plot that the enthalpy values for the Max_2-DNA formation were significantly higher than for either of the heterodimer-DNA interactions. This result suggests that the induced structural change by the Max homodimer-DNA complex is in contrast to heterodimer-DNA complex. Early study shows that in the Max_2-DNA crystal structure, the binding of the Max homodimer has been observed to bend DNA approximately 25 degrees toward the major groove and thus, towards the bound protein. But the DNA bends were not observed in Max-Mad or Max-c-Myc co-DNA crystal structures (28,60). The data herein supports this view and further suggests that the structural change not only occurs in high protein concentration, but in 100nM range,

which is close to the physiological condition. Further studies by energy transferring experiments also support the DNA bend during the protein binding (data not shown).

In addition, the anisotropy signals for the protein dimerization showed the difference on molecular size for these 3 dimers (Figure 15, page 54). The Max dimer has similar size as Max-Myc dimer, but the Max-Mad is much larger as expected. In contrast to Burley's group suggestion(60) on the formation of more complicated tetramer, there is no evidence to show the formation of tetramer in the protein concentration (under 2uM) in our experimental system. We suggest here that the formation of tetramer might only occur in higher concentration but not in physiological conditions. Cross-linking of the Max protein (60) might affect the protein-protein interaction.

The protein-binding pathway was studied by attempting to measure the equilibrium constants for all the interaction steps shown in Figure 6. The monomer-DNA binding measurement was limited due to the respectively small changes of the mean hydrodynamic volume V_h with or without DNA oligos (if protein is labeled and titration is performed by adding more DNA) and the monomer-DNA, dimer-DNA interaction happening spontaneously(if DNA is labeled and titration is performed by adding more protein). Instead of detecting this interaction in a Max only system, 2 heterodimer DNA systems were used to approach this problem and to proofread each other. In this heterodimer-binding assay, K_1, K_3 and K_4 were obtained directly from series of the titration experiments thus K_2 was calculated from the relationship:

$K_1 x K_3 = K_2 x K_4$

The results found that the binding affinity of Max monomer with DNA was about 20 to 50 folder tighter than the binding affinity for the heterodimerzation or homodimerization. It suggests that for the unphosphorylated Max, the dimerization and Protein-DNA interaction pathway might be favorable to the formation of Max monomer-DNA complex, instead of the formation of Max heterodimer. With such a strong binding ability with DNA but less functional domain in Max compact structure, Max monomer or dimer could easily anchored on the corresponded DNA elements and block the heterodimer communication with DNA. In this case, unphosphorylated Max protein is an ideal antagonist to the Myc protein. It has been already found that Max protein can be modified by phosphorylation. Phosphorylation of serines 2 and 11 of Max by casein kinase II impairs the DNA binding of Max-Max complexes (9,10). Although the structural effects of phosphorylation are not well known, it seems probable that the phosphorylation of the two serine residues would disrupt DNA-Protein interactions. Disruption may occur as a result of changes in the N-terminal cap of the binding helix of Max, and also as a result of charge repulsion. Thus the Max phosphorylation did not affect the heterodimer binding with DNA. Our result suggests a model that the Max phosphorylation by casein kinase II might be the core upstream regulation of the whole Myc/Max/Mad network by regulating the Max binding affinity with E-Box DNA.

In conclusion, by using analytical biophysical approach, especially by using fluorescence polarization and FRET, the quantitative data were obtained to establish the mechanism of the interaction among Myc/Max/Mad network. This work strongly support some of the view from the early qualitative research work, and also suggests the model of protein

dimerization and DNA binding, which apparently fits the data. FRET experiment also suggests the possible binding induced DNA structural change, which cause the different energy transfer for the Max homodimer and Max heterodimer with identical DNA oligos. Further research is needed. In addition, the fact that proteins such as Mga, Mxi1, Mlx, Mnt etc are all involved in this network by interacting with either Max or Myc, Mad *in vivo* increased the complexity. It is suggested that the system we applied here could be used as a experimental platform, by which a simple extra ligand (protein) would be added in as the research project. By this meaning, we might get a better understanding of this network.

APPENDIX

Appendix 1 Buffers used in the experiments

1.1 Cell media

LB media

NaCl	10g
Yeast Extract	5g
Peptone	10g
+ 1000ml	DDH_2O

1L LB media

SOC media

5M NaCl	2ml
Yeast Extract	5g
Peptone	20g
1M KCl	2.5ml
+	DD H_2O

1L SOC media

1.2 Reagents and solutions for cell cultivation

50mg/ml Ampicillin: 0.5g Ampicillin in 10ml DD H_2O

50mg/ml Kanamicin: 0.5g Kanamicin in 10ml DD H_2O

0.5 M IPTG: 1.62g IPTG in 12 ml DD H_2O

Protease inhibitor stock

Benzamidine HCl	40 mg
Phenanthroline	25 mg
Aprotinin	25 mg
Pepstatin A	25 mg
Leupeptin	25 mg
1xHEPES buffer	25ml
25ml 100xProtease inhibitor stock	

100mM PMSF: 440mg PMSF in 25ml isopropanol

1.3 Buffers for Protein purification and titrations

10X HEPES Buffer, pH7.6

HEPES	59.5g
KCl	74.6g
$MgCl_2$	2.0g
DTT*	
DD H_2O	900ml

Adjust pH to 7.6 by adding KOH, then fill DD H_2O till 1000 ml

* DTT adding finally to reach 10mM

Lysis Buffer

10X HEPES Buffer, pH7.6	10ml
Glycerol	10ml
Protease inhibitor stock	1ml
100mM PMSF	1ml
+78ml DD H_2O	

100ml Lysis Buffer

Dialysis Buffer (1X HEPES Buffer) 4000ml

Titration Buffer (1X HEPES Buffer)

1.4 Buffers for Electrophoresis

For DNA Agarose Gel

50x TAE buffer

Tris base	242g
EDTA	18.6 g
Glacial Acetic Acid	57.1ml
Adjust volume to 1L with DD H_2O	

6x DNA sample loading buffer

Bromophenol Blue	0.5ml
1.0%	4ml
Glycerol	0.2ml
50xTAE buffer	5.3ml
DD H_2O	
Totaling Volume	10ml

For Protein Gel

10xTank buffer

Tris base	24.22g
SDS	10g
Glycine	144.40g
Adjust volume to 1L with DD H_2O	

4xResolving Gel buffer (1M Tris-Cl buffer pH8.8)

4xStacking Gel buffer (0.5M Tris-Cl buffer pH6.8)

6xProtein Sample Lording buffer

4xStacking Gel buffer	1.56ml
SDS	1.0g
Glycerol	5.0ml
Bromphenol blue 1.0%	0.5ml
β-mercaptoethanol	2.5ml
+ DD H_2O	0.44ml
Totaling Volume	10ml

Appendix 2 PROTEIN PURIFICATION AND DETECTING

2.1 Max protein purification by using Hightrap SP column

Gradient Buffers for Hightrap SP column

	Buffer A	**Buffer B**
2M KCl	6.25ml	100ml
10X HEPES Buffer, pH7.6	50ml	20ml
0.5M EDTA, pH8.0	0.5ml	0.2ml
100mM PMSF	1ml in 200ml A	1ml
Glycerol	50ml	20ml
Octyl Glycoside	1g in 200ml A	1g
DD H_2O	Fill to 500ml	Fill to 200ml
Totaling	500ml	200ml

Link the Hightrap SP column

↓

Elute the column with buffers. The buffer using in the elution process is followed the sequences:

(a) 20ml Buffer A, 5ml/min
(b) 50ml Buffer A, 2ml/min
(c) 50ml Buffer A + 1M NaCl, 2ml/min
(d) 50ml buffer A, 2ml/min
(e) Protein Sample, 2ml/min
(f) 30ml Buffer A (+ Octyl Glycoside, + PMSF), 2ml/min
(g) 30ml 70% Buffer A(21ml) and 30% Buffer B(9ml) , 2ml/min
(h) 140ml 40% Buffer A (56ml) and 60% Buffer B (84ml), 2ml/min
(i) 40ml 20% Buffer A (8ml) and 80% Buffer B (32ml), 5ml/min
(j) 65ml Buffer A + 1M NaCl, 5ml/min
(k) 50ml Buffer A, 5ml/min

↓

Collect the all fractions in to 1.5ml tubes (20 drops each).

↓

Transfer fraction 3 to dialysis tubing and dialyze against 1X HEPES Buffer overnight in 4°C.

↓

Estimate protein concentration and detect the purity by SDS-PAGE

↓

Transfer proteins to Centricon Tubes and centrifuge at 5000rpm for 3 hours. Detect the final protein concentration by Bradford methods.

2.2 Mad protein purification by using the His-tag affinity column

The buffers for His-tag affinity column include:

Binding Buffer: 0.5M NaCl, 20mM Tris-HCl, 5mM imidazole, pH 7.9
Wash Buffer: 0.5M NaCl, 60mM imidazole, 20mM Tris-HCl, pH 7.9
Elute Buffer: 1M imidazole, 0.5M NaCl, 20mM Tris-HCl, pH 7.9
Strip Buffer: 0.5M NaCl, 100mM EDTA, 20mM Tris-HCl, pH 7.9
Charge Buffer: 50mM NiSO4

The protocols used here is as following:

Load 1ml His-Bind resin (from Novagen) to the 5ml sized chromatography column

Load 10ml of binding buffer to wash the column

Load 5ml Charge buffer to charge the column with Ni^{2+}

Load 10ml of Binding Buffer to wash the column

Load the protein samples in Nickel charged His-trap column

Wash the column with 10ml binding buffer

Wash the column with 10ml wash buffer

Elute the column with 10ml Elute Buffer and start to collect the fractions (20 drops per tubes)

Estimate protein concentration and detect the purity by SDS-PAGE. Transfer fractions with desired proteins to dialysis tubing and dialyze against 1X HEPES Buffer (without DTT) overnight in 4°C. Transfer proteins to Centricon Tubes and centrifuge at 5000rpm for 3 hours. Detect the final protein concentration by Bradford methods

2.3 Myc protein purification by GST affinity column

The buffers for GST affinity column include:

10xGST Bind/Wash Buffer: 10x = 43 mM Na2HPO4, 14.7 mM KH2PO4, 1.37 M NaCl, 27 mM KCl, pH 7.3

10xGST Elution Buffer: 10x = 500 mM Tris-HCl, 100mM Reduced Glutathione, pH 8.0

The Protocols used in the experiments are as following:

Gently load 1ml GST•Bind Resin (from Novagen) to small polypropylene columns (5ml size)

Wash the resin with 10ml of GST Bind/Wash Buffer

Load the column with the prepared protein extract

Wash the column with 10ml 1X GST Bind/Wash Buffer.

Elute the bound protein with 5ml of 1X GST Elution Buffer. Start to collect the fractions (20 drops per tubes)

Estimate protein concentration and detect the purity by SDS-PAGE. Transfer fractions with desired proteins to dialysis tubing and dialyze against 1X HEPES Buffer (without DTT) overnight in 4°C. Transfer proteins to Centricon Tubes and centrifuge at 5000rpm for 3 hours. Detect the final protein concentration by Bradford methods

2.4 Determine the protein concentration by Bradford Method

The Scheme of Bradford method to determine the protein concentration is by the Coomassie® - Protein Reaction

Protein + Coomassie® G-250 in an acidic medium →Protein-Dye complex (blue color, *measured at 595 nm*)

The protocols used in this experiment are as following:

1. Preparation of Diluted BSA Standards

Prepare a fresh set of protein standards by diluting the 2.0 mg/ml BSA stock standard (Stock) (preferably in the same diluent as your samples) as illustrated in Table below. 1 ml 2.0 mg/ml BSA standard is sufficient to prepare a set of diluted standards for either working range.

Table: Preparation of the Diluted BSA Standards
Standard Test Tube or Plate Protocol, Working Range = 100 - 1500 µg/ml

Volume of the BSA to Add	Volume of Diluent to Add	Final BSA Concentration
300 µl of (Stock)	0 µl	2,000 µg/ml
375 µl of (Stock)	125 µl	1,500 µg/ml (A)
325 µl of (Stock)	325 µl	1,000 µg/ml (B)
175 µl of (A)	175 µl	750 µg/ml (C)
325 µl of (B)	325 µl	500 µg/ml (D)
325 µl of (D)	325 µl	250 µg/ml (E)
325 µl of (E)	325 µl	125 µg/ml (F)
100 µl of (F)	400 µl	25 µg/ml (G)

2. Mixing of the Coomassie® Plus Protein Assay Reagent

Allow the Coomassie® Plus Reagent to come to room temperature. Mix the Coomassie® Plus Reagent solution just prior to use by gently inverting the bottle several times. Do not shake.

3. Reaction

Pipet 0.05 ml of each standard or unknown sample into appropriately labeled UV cuvette. Use 0.05 ml of the diluent for the blank. Add 1.5 ml of the Coomassie® Plus Reagent to each tube, mix well.

4.Detection

Switch on the Cary UV linked computer. Open the [Concentration] program on the windows desktop. Measure the absorbance at 595 nm of blank and zero the Cary UV reading. Measure the absorbance at 595 nm of each cuvette. Prepare a standard curve by plotting the average blank corrected 595 nm reading for each BSA standard versus its concentration in μg/ml. Using the standard curve, determine the protein concentration for each unknown sample.

2.5 SDS Polyacrylamide Gel Electrophoresis (SDS-PAGE)

Assembling gel apparatus:

Assemble one glass plate and one aluminum plate with two side spacers and two clamps. Stand assembly upright using clamps as supports, on glass plate. Pour some pre-heated 2% Agarose (2% Agarose in 0.5M NaCl solution) onto glass plate, place assembly in pool of agarose: this seals the bottom of the assembly.

1) Resolving Gels:

Gel concentration of 12% in 0.25 M Tris-HCl pH 8.8

Reagent:	Volume (ml: TO MAKE 5 ML)	Volume (ml: TO MAKE 10 ML)
30% Acrylamide stock*:	2.0	4.0
water (distilled)	1.5	3.2
1 M Tris-HCl pH 8.8	1.3	2.5
10% SDS	0.1	0.2
Ammonium Persulphate 10%	0.1	0.1
TEMED (added last)	5µL	5µL

* = 29:1 w:w ratio of acrylamide to N,N'-methylene bis-acrylamide

Mix ingredients very carefully in the order shown above, ensuring no air bubbles form. Pour into glass plate assembly. Overlay gel with isopropanol to ensure a flat surface and to exclude air. Wash off isopropanol with water after gel has polymerized (about15 min).

2) Stacking Gels:

Gel concentration of 5% in 0.125 M Tris-HCl pH 6.8

Reagent:	Volume (ml: TO MAKE 5 ML)	Volume (ml: TO MAKE 10 ML)
30% Acrylamide stock*:	0.83	1.66
water (distilled)	2.72	5.54
0.5 M Tris-HCl pH 8.8	1.25	2.5
10% SDS	0.1	0.2
Ammonium Persulphate 10%	0.1	0.1
TEMED (added last)	5µL	5µL

Mix as before, then pour onto top of set resolving gel, insert comb, allow to polymerize (about 30 minutes), remove comb, fill with electrophoresis buffer. Assemble top tank onto glass plate assembly. Fill with electrophoresis buffer.

3) Electrophoresis buffer

The final TANK buffer composition is 196mM glycine / 0.1% SDS / 50mM Tris-HCl pH 8.3, made by diluting a 10x stock solution. This goes in both top and bottom tanks.

4) The protein samples:

Take supernatant and mix 50μL 1:1 (v:v) with SDS-PAGE disruption mix: this is 125mM Tris-HCl pH 6.8 / 10% 2-mercaptoethanol / 10% SDS / 10% glycerol, containing a little bromophenol blue. For liquid / purified samples, take e.g. 100 μL and add 50 - 100 μL of disruption mix.

Heat sample Eppendorfs for 5 min at boiling water in a "float" in a water bath then sat on ice for 10 minutes. Layer samples under buffer into wells on stacking gels. Connect up apparatus and electrophorese to the power supply. Set Voltage as 150V and current as 20mA.

5) Stain the gel by using Coomassie Brilliant Blue R250

Make up stain: 0.2% Coomassie Brilliant Blue R250 in 45% 45% 10 % methanol water acetic acid. Cover gel with staining solution, seal in plastic box and leave overnight on shaker (RT) or for 2 to 3 hours at 37 c also with agitation.

Destain with 25% 65% 10% methanol water acetic acid mix, with agitation. Change the distaining solution several times until the gel background color goes transparent..

Appendix 3 SOME MOLECULAR CLONING PROTOCOLS USED IN THESE EXPERIMENTS

3.1. QIAprep Spin Miniprep Kit Protocol to extract and purify the plasmid DNA

The following buffers are applied in this experiment:

Buffers: P1, RNase A has to be added before usage
P2
N3
PB
PE, before use, 24ml ethanol has to be added to obtain 30ml buffer PE

The following protocols are following the QIAprep Spin Miniprep Kit Manual with slight modifications to fit my experiments:

Pellet the 5ml overnight-incubated *E.coli* grown in LB medium by centrifugation at 5000 rpm for 10 minutes.

↓

Resuspend pelleted bacterial cells in 250 μl Buffer P1 (precooled in 4°C) and transfer to a microcentrifuge tube. Ensure that RNase A has been added to Buffer P1. No cell clumps should be visible after resuspension of the pellet.

↓

Add 250 μl Buffer P2 and invert the tube gently 4–6 times to mix. Do not vortex, as this will result in shearing of genomic DNA. If necessary, continue inverting the tube until the solution becomes viscous and slightly clear. Do not allow the lysis reaction to proceed for more than 5 min.

↓

Add 350 µl Buffer N3 and invert the tube immediately but gently 4–6 times. To avoid localized precipitation, immediately after addition of Buffer N3 mix the solution gently but thoroughly. The solution should become cloudy.

↓

Centrifuge for 10 min at 12,000 rpm in microcentrifuge. A compact white pellet will form.

↓

Apply the supernatant from step 4 to the QIAprep Spin Column. Switch on vacuum source to draw the solution through the QIAprep Spin Columns, and then switch off vacuum source.

↓

Wash the QIAprep Spin Column by adding 0.5 ml Buffer PB. Switch on vacuum source. After the solution has moved through the column, switch off vacuum source. This step is necessary to remove trace nuclease activity

↓

Wash the QIAprep Spin Column by adding 0.75 ml Buffer PE. Switch on vacuum source to draw the wash solution through the column, and then switch off vacuum source.

↓

Transfer the QIAprep Spin Columns to a microcentrifuge tube. Centrifuge for 1 min. This extra spin is to remove residual Buffer PE. Residual ethanol from Buffer PE may inhibit future enzymatic reactions.

↓

Place the QIAprep column in a clean 1.5 ml microcentrifuge tube. To elute DNA, add Nuclease free water to the center of the QIAprep Spin Column, let stand for 1 min, and centrifuge for 1 min.

↓

Take 8μL of the filtrate and mix with 2μL DNA sample loading buffer. Load the mix in the Agarose Gel and detect the DNA after running the Gel.

3.2. QIAquick PCR Purification Kit Protocol to purify the PCR products

Buffers: PB
PE, before use, 24ml ethanol has to be added to obtain 30ml buffer PE

The following protocols are following the QIAquick PCR Purification Kit Manual with slight modifications to fit my experiments:

Add 5 volumes of Buffer PB to 1 volume of the PCR sample and mix. For example, add 500 µl of Buffer PB to 100 µl PCR sample (not including oil).

↓

To bind DNA, load the samples into the QIAquick columns, and apply vacuum. After the samples have passed through the column, switch off the vacuum source. The maximum loading volume of the column is 800 µl. For sample volumes greater than 800 µl simply load again.

↓

To wash, add 0.75 ml of Buffer PE to each QIAquick column and apply vacuum.

↓

Transfer each QIAquick column to a microcentrifuge tube or the provided 2 ml collection tubes. Centrifuge for 1 min at 13,000 rpm. This spin is necessary to remove residual ethanol (Buffer PE).

↓

Place each QIAquick column into a clean 1.5 ml microcentrifuge tube. To elute DNA, add 30 µl of nuclease free water to the center of each QIAquick membrane. Let the columns stand for 1 min, and then centrifuge the columns for 1 min at 13,000 rpm.

3.3. DNA Agarose Gel Electrophoresis

1) Preparation of Agarose solution

To prepare 100 ml of a 0.8% agarose solution, measure 0.8g agarose into a glass beaker or flask and add 100 ml 1X TAE. Microwave for about 2 minutes until agarose is dissolved and solution is clear.

↓

Allow solution to cool to about 60°C before pouring. 10µl Ethidium bromide (5mg/ml stock) is added to the gel solution at this point to make the final concentration of 0.5 µg/ml.

2) Preparation of Agarose Gel

Prepare gel tray by sealing both ends with tapes. Place comb in gel tray about 1 inch from one end of the tray and position the comb vertically such that the teeth are about 1-2 mm above the surface of the tray.

↓

Pour Agarose gel solution into tray to a depth of about 5 mm. Allow gel to solidify about 30 minutes at room temperature.

3) Preparation of DNA samples

Add 1 µl of 6x gel loading dye (see appendix 1) for every 5 µl of DNA solution. Mix well. Load 5-12 µl of DNA per well.

4) Run the Gel

To run, gently remove the comb, place tray in electrophoresis chamber, and cover (just until wells are submerged) with electrophoresis buffer (the same buffer used to prepare the agarose).

↓

Electrophorese at 100 volts until dye markers have migrated an appropriate distance, depending on the size of DNA to be visualized. In this experiments, dye marker only needs to run to the 2/3-gel distance for the PCR products.

5) Detect the result

Place the gel on the transilluminator. Place the clear plastic shield over the transilluminator window before turning on the UV light. Turn on the transilluminator and look at the gel. Confirm the presence of DNA (orange bands) and turn off the transilluminator.

3.4. Ligation reaction with Novagen® Clonables 2X Ligation Premix

This kit contains components sufficient for 11 ligation and transformation reactions:

Components: 55 µl Clonables 2X Ligation Premix
10 µl Clonables Positive Control
1.5 ml Nuclease-free Water
11 x 50 µl NovaBlue Singles Competent Cells
2 x 2 ml SOC Medium
1 Test Plasmid

The following procedures are based on the Novagen® Clonables 2X Ligation Premix manual with slight modification to fit our experiment:

The digested pET30a plasmid was purified by using the QIAquick® spin column (protocol in Appendix 3.1)

↓

The digested cDNA PCR product was purified by using the QIAquick® PCR purification column (protocol in Appendix 3.2)

↓

Assembly the ligation reaction mixture as indicated in the table below:

pET30a	1µL
PCR Product	2µL
Nuclease free water	2µL
2xligation premix	5µL
Totaling Volume	10µL

Place the mixture in room temperature for 30 minutes and then place it on ice

↓

Thaw 3 tubes of competent cells (1 tube for negative control, 1 tube for positive control and 1 tube for the ligation products) on ice and mix gently to ensure that the cells are evenly suspended.

↓

Add 1 µl of the ligation reaction directly to the cells. Stir gently to mix. For the positive control, 0.5µL pET30a plasmid is added.

↓

Place the tubes on ice for 5 min. Then heat the tubes for exactly 30 sec in a 42°C water bath; do not shake.

↓

Place the tubes on ice for 2 min. Add 250 µl of room temperature SOC medium to each tube. Shake at 37°C (250 rpm) for 30 min prior to plating on LB agar containing 30µg/ml kanamycin).

BIBLIOGRAPHY

1. Amati, B.; Brooks, M. W.; Levy, N.; Littlewood, T. D.; Evan, G. I.; Land, H. *Cell* 1993, *72*(2), 233-245.

2. Amati, B.; Dalton, S.; Brooks, M. W.; Littlewood, T. D.; Evan, G. I.; Land, H. *Nature* 1992, *359*(6394), 423-426.

3. Amati, B.; Land, H. *Curr.Opin.Genet.Dev.* 1994, *4*(1), 102-108.

4. Amati, B.; Littlewood, T. D.; Evan, G. I.; Land, H. *EMBO J.* 1993, *12*(13), 5083-5087.

5. Armelin, H. A.; Armelin, M. C.; Kelly, K.; Stewart, T.; Leder, P.; Cochran, B. H.; Stiles, C. D. *Nature* 1984, *310*(5979), 655-660.

6. Askew, D. S.; Ashmun, R. A.; Simmons, B. C.; Cleveland, J. L. *Oncogene* 1991, *6*(10), 1915-1922.

7. Ayer, D. E.; Eisenman, R. N. *Genes Dev.* 1993, *7*(11), 2110-2119.

8. Ayer, D. E.; Kretzner, L.; Eisenman, R. N. *Cell* 1993, *72*(2), 211-222.

9. Berberich, S.; Cole, M. D. *Genes Dev.* 1992, *6*(2), 166-176.

10. Berberich, S.; Hyde-DeRuyscher, N.; Espenshade, P.; Cole, M. D. *Oncogene* 1992, *7*(4), 775-779.

11. Billin, A. N.; Eilers, A. L.; Coulter, K. L.; Logan, J. S.; Ayer, D. E. *Mol.Biol.Cell* 2000, *20*(23), 8845-8854.

12. Billin, A. N.; Eilers, M.; Queva, C.; Ayer, D. E. *J.Biol.Chem.* 1999, *274*(51), 36344-36350.

13. Blackwell, T. K.; Huang, J.; Ma, A.; Kretzner, L.; Alt, F. W.; Eisenman, R. N.; Weintraub, H. *Mol.Cell Biol.* 1993, *13*(9), 5216-5224.

14. Blackwood, E. M.; Eisenman, R. N. *Science* 1991, *251*(4998), 1211-1217.

15. Blackwood, E. M.; Luscher, B.; Kretzner, L.; Eisenman, R. N. *Cold Spring Harb.Symp.Quant.Biol.* 1991, *56* 109-117.

16. Bouchard, C.; Dittrich, O.; Kiermaier, A.; Dohmann, K.; Menkel, A.; Eilers, M.; Luscher, B. *Genes Dev.* 2001, *15*(16), 2042-2047.

17. Bradford, M. M. *Anal.Biochem* 1976, *72* 248-254.

18. Bresnick, E. H.; Felsenfeld, G. *J.Biol.Chem.* 1993, *268*(25), 18824-18834.

19. Cairo, S.; Merla, G.; Urbinati, F.; Ballabio, A.; Reymond, A. *Hum.Mol.Genet.* 2001, *10*(6), 617-627.

20. Cheng, S. W.; Davies, K. P.; Yung, E.; Beltran, R. J.; Yu, J.; Kalpana, G. V. *Nat.Genet.* 1999, *22*(1), 102-105.

21. Cheung, P.; Allis, C. D.; Sassone-Corsi, P. *Cell* 2000, *103*(2), 263-271.

22. Cole, M. D. *Basic Life Sci.* 1986, *38* 399-406.

23. Cole, M. D. *Annu.Rev.Genet.* 1986, *20* 361-384.

24. Dang, C. V. *Mol.Biol.Cell* 1999, *19*(1), 1-11.

25. Eisenman, R. N.; Hann, S. R. *Proc.R.Soc.Lond B Biol.Sci.* 1985, *226*(1242), 73-78.

26. Eisenman, R. N.; Tachibana, C. Y.; Abrams, H. D.; Hann, S. R. *Mol.Cell Biol.* 1985, *5*(1), 114-126.

27. Evan, G.; Harrington, E.; Fanidi, A.; Land, H.; Amati, B.; Bennett, M. *Philos.Trans.R.Soc.Lond B Biol.Sci.* 1994, *345*(1313), 269-275.

28. Ferre-D'Amare, A. R.; Pognonec, P.; Roeder, R. G.; Burley, S. K. *EMBO J.* 1994, *13*(1), 180-189.

29. Ferre-D'Amare, A. R.; Prendergast, G. C.; Ziff, E. B.; Burley, S. K. *Nature* 1993, *363*(6424), 38-45.

30. Foley, K. P.; McArthur, G. A.; Queva, C.; Hurlin, P. J.; Soriano, P.; Eisenman, R. N. *EMBO J.* 1998, *17*(3), 774-785.

31. Freytag, S. O.; Dang, C. V.; Lee, W. M. *Cell Growth Differ.* 1990, *1*(7), 339-343.

32. Fry, C. J.; Peterson, C. L. *Curr.Biol.* 2001, *11*(5), R185-R197.

33. Goodrich, J. A.; Cutler, G.; Tjian, R. *Cell* 1996, *84*(6), 825-830.

34. Grandori, C.; Cowley, S. M.; James, L. P.; Eisenman, R. N. *Annu.Rev.Cell Dev.Biol.* 2000, *16* 653-699.

35. Gregory, M. A.; Hann, S. R. *Mol.Biol.Cell* 2000, *20*(7), 2423-2435.

36. Gupta, S.; Anand, G.; Yin, X.; Grove, L.; Prochowinik, E. V. *Oncogene* 1998, *16*(9), 1149-1159.

37. Hann, S. R.; Abrams, H. D.; Rohrschneider, L. R.; Eisenman, R. N. *Cell* 1983, *34*(3), 789-798.

38. Hann, S. R.; Eisenman, R. N. *Mol.Cell Biol.* 1984, *4*(11), 2486-2497.

39. Henriksson, M.; Bakardjiev, A.; Klein, G.; Luscher, B. *Oncogene* 1993, *8*(12), 3199-3209.

40. Henriksson, M.; Luscher, B. *Adv.Cancer Res.* 1996, *68* 109-182.

41. Hurlin, P. J.; Foley, K. P.; Ayer, D. E.; Eisenman, R. N.; Hanahan, D.; Arbeit, J. M. *Oncogene* 1995, *11*(12), 2487-2501.

42. Hurlin, P. J.; Queva, C.; Eisenman, R. N. *Genes Dev.* 1997, *11*(1), 44-58.

43. Hurlin, P. J.; Queva, C.; Eisenman, R. N. *Curr.Top.Microbiol.Immunol.* 1997, *224* 115-121.

44. Hurlin, P. J.; Queva, C.; Koskinen, P. J.; Steingrimsson, E.; Ayer, D. E.; Copeland, N. G.; Jenkins, N. A.; Eisenman, R. N. *EMBO J.* 1995, *14*(22), 5646-5659.

45. Hurlin, P. J.; Steingrimsson, E.; Copeland, N. G.; Jenkins, N. A.; Eisenman, R. N. *EMBO J.* 1999, *18*(24), 7019-7028.

46. James, L.; Eisenman, R. N. *Proc.Natl.Acad.Sci.U.S.A* 2002, *99*(16), 10429-10434.

47. Kato, G. J.; Lee, W. M.; Chen, L. L.; Dang, C. V. *Genes Dev.* 1992, *6*(1), 81-92.

48. Kerkhoff, E.; Bister, K. *Oncogene* 1991, *6*(1), 93-102.

49. Kiermaier, A.; Eilers, M. *Curr.Biol.* 1997, *7*(8), 505-507.

50. Kingston, R. E.; Narlikar, G. J. *Genes Dev.* 1999, *13*(18), 2339-2352.

51. Knoepfler, P. S.; Eisenman, R. N. *Cell* 1999, *99*(5), 447-450.

52. Kohler, J. J.; Schepartz, A. *Biochemistry* 2001, *40*(1), 130-142.

53. Kornberg, R. D.; Lorch, Y. *Cell* 1999, *98*(3), 285-294.

54. Kretzner, L.; Blackwood, E. M.; Eisenman, R. N. *Nature* 1992, *359*(6394), 426-429.

55. Lakowicz, J. R.; Maliwal, B. P.; Cherek, H.; Balter, A. *Biochemistry* 1983, *22*(8), 1741-1752.

56. Littlewood, T. D.; Amati, B.; Land, H.; Evan, G. I. *Oncogene* 1992, *7*(9), 1783-1792.

57. Marcu, K. B.; Bossone, S. A.; Patel, A. J. *Annu.Rev.Biochem.* 1992, *61* 809-860.

58. McMahon, S. B.; Wood, M. A.; Cole, M. D. *Mol.Biol.Cell* 2000, *20*(2), 556-562.

59. Meroni, G.; Cairo, S.; Merla, G.; Messali, S.; Brent, R.; Ballabio, A.; Reymond, A. *Oncogene* 2000, *19*(29), 3266-3277.

60. Nair, S. K.; Burley, S. K. *Cell* 2003, *112*(2), 193-205.

61. Niklinski, J.; Claassen, G.; Meyers, C.; Gregory, M. A.; Allegra, C. J.; Kaye, F. J.; Hann, S. R.; Zajac-Kaye, M. *Mol.Biol.Cell* 2000, *20*(14), 5276-5284.

62. Novagen . His•Tag® & GST•Tag™ Purification and Detection Tools . 2003.

63. O'Hagan, R. C.; Ohh, M.; David, G.; de Alboran, I. M.; Alt, F. W.; Kaelin, W. G., Jr.; DePinho, R. A. *Genes Dev.* 2000, *14*(17), 2185-2191.

64. Peterson, C. L.; Workman, J. L. *Curr.Opin.Genet.Dev.* 2000, *10*(2), 187-192.

65. Prendergast, G. C.; Lawe, D.; Ziff, E. B. *Cell* 1991, *65*(3), 395-407.

66. Pulverer, B.; Fisher, C.; Vousden, K.; Littlewood, T. D.; Evan, G.; Woodgett, J. R. *Oncogene* 1994, *9*(1), 59-70.

67. Queva, C.; Hurlin, P. J.; Foley, K. P.; Eisenman, R. N. *Oncogene* 1998, *16*(8), 967-977.

68. Queva, C.; McArthur, G. A.; Iritani, B. M.; Eisenman, R. N. *Mol.Cell Biol.* 2001, *21*(3), 703-712.

69. Queva, C.; McArthur, G. A.; Ramos, L. S.; Eisenman, R. N. *Cell Growth Differ.* 1999, *10*(12), 785-796.

70. Roussel, M. F.; Ashmun, R. A.; Sherr, C. J.; Eisenman, R. N.; Ayer, D. E. *Mol.Cell Biol.* 1996, *16*(6), 2796-2801.

71. Sakamuro, D.; Prendergast, G. C. *Oncogene* 1999, *18*(19), 2942-2954.

72. Schreiber-Agus, N.; DePinho, R. A. *Bioessays* 1998, *20*(10), 808-818.

73. Sha, M.; Ferre-D'Amare, A. R.; Burley, S. K.; Goss, D. J. *J.Biol.Chem.* 1995, *270*(33), 19325-19329.

74. Solomon, D. L.; Amati, B.; Land, H. *Nucleic Acids Res.* 1993, *21*(23), 5372-5376.

75. Strahl, B. D.; Allis, C. D. *Nature* 2000, *403*(6765), 41-45.

76. Struhl, K. *Cell* 1996, *84*(2), 179-182.

77. Tada, M.; Smith, J. C. *Dev.Growth Differ* 2001, *43*(1), 1-11.

78. Wei, C. C.; Balasta, M. L.; Ren, J.; Goss, D. J. *Biochemistry* 1998, *37*(7), 1910-1916.

79. Wolffe, A. P.; Hansen, J. C. *Cell* 2001, *104*(5), 631-634.

80. Yin, X.; Gupta, K.; Han, W. P.; Levitan, E. S.; Prochowinik, E. V. *Oncogene* 1999, *18*(48), 6621-6634.

81. Zervos, A. S.; Gyuris, J.; Brent, R. *Cell* 1994, *79*(2), following.